ATMOSPHERIC OPTICS GROUP
TECHNICAL NOTE NO. 265

May 2004

Project Report for Providing Two Day/Night Whole Sky Imagers And Related Development Work For Starfire Optical Range

Published as Final Report for ONR Contract
N00014-97-D-0350 DO #6

UNIVERSITY OF CALIFORNIA SAN DIEGO

SCRIPPS INSTITUTION OF OCEANOGRAPHY

Janet E. Shields
Monette E. Karr
Art R. Burden
Richard W. Johnson
Justin G. Baker

The material contained in this note is to be considered proprietary in nature and is not authorized for distribution without the prior consent of the Marine Physical Laboratory.

MARINE PHYSICAL LAB San Diego, CA 92152-6400

Project Report for Providing Two Day/Night Whole Sky Imagers And Related Development Work For Starfire Optical Range

Published as Final Report for ONR Contract
N00014-97-D-0350 DO #6

Janet E. Shields, Monette E. Karr, Art R. Burden,
Richard W. Johnson, and Justin G. Baker

REPORT DOCUMENTATION PAGE

Form Approved OMB No. 0704-0188

Public reporing burden for this collection of information is estimated to average 1 hour per response, including the time for reviewing instructions, searching existing data sources, gathering and maintaining the data need ed, and completing and reviewing the collection of information. Send comments regarding this burden estimate or any other aspect of this collection of information, including suggestions for reducing this burden, to Washington Headquarters Services, Directorate for information Operations and Reports, 1215 Jefferson Davis Highway, Suite 1204, Arlington, VA 22202-4302, and to the Office of Management and Budget, Paperwork Reduction Project (0704-0188), Washington, DC 20503.

1. Agency Use Only (Leave Blank).	2. Report Date. May 27, 2004	3. Report Type and Dates Covered. Final Report

4. Title and Subtitle.
Project Report for Providing Two Day/Night Whole Sky Imagers and Related Development Work for Starfire Optical Range

5. Funding Numbers.
N00014-97-D-0350-D06

6. Author(s).
Janet E. Shields, Monette E. Karr, Art R. Burden, Richard W. Johnson, and Justin G. Baker

Project No.
Task No.

7. Performing Monitoring Agency Names(s) and Address(es).
University of California, San Diego
Marine Physical Laboratory
Scripps Institution of Oceanography
291 Rosecrans Street
San Diego, CA 92106

8. Performing Organization Report Number.

9. Sponsoring/Monitoring Agency Name(s) and Address(es).
Office of Naval Research
Department of the Navy
800 North Quincy Street
Arlington, VA 22217-5660
Atten: CDR Dale Lichtey, Code 321

10. Sponsoring/Monitoring Agency Report Number.

11. Supplementary Notes.

12a. Distribution/Availability Statement.
Approved for public release; distribution is unlimited.

12b. Distribution Code.

13. Abstract (Maximum 200 words).
This report documents the work performed for Starfire Optical Range under Contract N00014-97-D-0350-D06. Under this contract the Atmospheric Optics Group at the Marine Physical Laboratory, Scripps Institution of Oceanography, University of California, San Diego, developed and built two Day/Night Whole Sky Imagers (WSI), developed code and methodology for real-time processing of the data, developed a night cloud algorithm, and provided other related work.

14. Subject Terms.
atmospheric optics, Whole Sky Imager

15. Number of Pages.
19

16. Price Code.

17. Security Classification of Report.	18. Security Classification of This Page.	19. Security Classification of Abstract..	20. Limitation of Abstract.
Unclassified	Unclassified	Unclassified	None

REPORT DOCUMENTATION PAGE

Form Approved OMB No. 0704-0188

Public reporing burden for this collection of information is estimated to average 1 hour per response, including the time for reviewing instructions, searching existing data sources, gathering and maintaining the data need ed, and completing and reviewing the collection of information. Send comments regarding this burden estimate or any other aspect of this collection of information, including suggestions for reducing this burden, to Washington Headquarters Services, Directorate for information Operations and Reports, 1215 Jefferson Davis Highway, Suite 1204, Arlington, VA 22202-4302, and to the Office of Management and Budget, Paperwork Reduction Project (0704-0188), Washington, DC 20503.

1. Agency Use Only (Leave Blank).	2. Report Date. May 27, 2004	3. Report Type and Dates Covered. Final Report

4. Title and Subtitle.

Project Report for Providing Two Day/Night Whole Sky Imagers and Related Development Work for Starfire Optical Range

5. Funding Numbers.

N00014-97-D-0350-D06

Project No.

Task No.

6. Author(s).

Janet E. Shields, Monette E. Karr, Art R. Burden, Richard W. Johnson, and Justin G. Baker

7. Performing Monitoring Agency Names(s) and Address(es).

University of California, San Diego
Marine Physical Laboratory
Scripps Institution of Oceanography
291 Rosecrans Street
San Diego, CA 92106

8. Performing Organization Report Number.

9. Sponsoring/Monitoring Agency Name(s) and Address(es).

Office of Naval Research
Department of the Navy
800 North Quincy Street
Arlington, VA 22217-5660
Atten: CDR Dale Lichtey, Code 321

10. Sponsoring/Monitoring Agency Report Number.

11. Supplementary Notes.

12a. Distribution/Availability Statement.

Approved for public release; distribution is unlimited.

12b. Distribution Code.

13. Abstract (Maximum 200 words).

This report documents the work performed for Starfire Optical Range under Contract N00014-97-D-0350-D06. Under this contract the Atmospheric Optics Group at the Marine Physical Laboratory, Scripps Institution of Oceanography, University of California, San Diego, developed and built two Day/Night Whole Sky Imagers (WSI), developed code and methodology for real-time processing of the data, developed a night cloud algorithm, and provided other related work.

14. Subject Terms.

atmospheric optics, Whole Sky Imager

15. Number of Pages. 19

16. Price Code.

17. Security Classification of Report.	18. Security Classification of This Page.	19. Security Classification of Abstract..	20. Limitation of Abstract.
Unclassified	Unclassified	Unclassified	None

ONR/MPL REPORT DISTRIBUTION

Office of Naval Research (3)
Department of the Navy
Ballston Tower One
800 North Quincy Street
Arlington, VA 22217-5660
Atten: CDR Dale Lichtey, Code 321

Regional Director (1)
ONR Detachment
San Diego Regional Office
4520 Executive Drive, Suite 300
San Diego, CA 92121-3019

Commanding Officer (1)
Naval Research Laboratory
4555 Overlook Avenue, S.W.
Attn: Code 2627
Washington, D.C. 20375-5320

Defense Technical Information Center (4)
8725 John J. Kingman Road
Suite 0944
Ft. Belvoir, VA 22060-6218

ONR/MPL REPORT DISTRIBUTION

Office of Naval Research (3)
Department of the Navy
Ballston Tower One
800 North Quincy Street
Arlington, VA 22217-5660
Atten: CDR Dale Lichtey, Code 321

Regional Director (1)
ONR Detachment
San Diego Regional Office
4520 Executive Drive, Suite 300
San Diego, CA 92121-3019

Commanding Officer (1)
Naval Research Laboratory
4555 Overlook Avenue, S.W.
Attn: Code 2627
Washington, D.C. 20375-5320

Defense Technical Information Center (4)
8725 John J. Kingman Road
Suite 0944
Ft. Belvoir, VA 22060-6218

Project Report for Providing Two Day/Night Whole Sky Imagers And Related Development Work For Starfire Optical Range

Table of Contents

Figures

Attachments

Project Report for
Providing Two Day/Night Whole Sky Imagers
And Related Development Work
For Starfire Optical Range

**Janet E. Shields, Monette E. Karr, Art R. Burden,
Richard W. Johnson, and Justin G. Baker**

1. Introduction

This report documents the work performed for Starfire Optical Range under Contract N00014-97-D-0350 DO #6. Under this contract, the Atmospheric Optics Group at the Marine Physical Lab, Scripps Institution of Oceanography, University of California San Diego, developed and built two Day/Night Whole Sky Imagers (WSI), developed code and methodology for real-time processing of the data, developed a night cloud algorithm, and provided other related work.

MPL has been developing WSIs since the early 1980's (Johnson 1989, 1991). The first Day/Night WSIs with 24-hour a day capability were initially developed and deployed in the early 1990's. The D/N WSI instruments have been significantly upgraded in capability since that time (Shields 1993, 1998). One of the early instruments, Day/Night WSI Unit 2, was delivered to the Air Force Starfire Optical Range in October 92. This work was funded by the Air Force Phillips Lab under Contract N00014-89-D-0142 DO #18 (Shields 1994).

For several years, the WSI was operated at SOR without significant interaction from MPL. Then in 1997, MPL was funded under Contract N00014-97-D-0350 DO #02 to develop and field a new D/N WSI (Unit 12), as well as provide analysis of Cloud Free Line of Sight (CFLOS) statistics from an earlier WSI database. This work was reported in Shields et al. 2003a and 2003b.

Partly as a result of this work, MPL was funded under the present contract to provide two more D/N WSI units, (Units 13 and 14) and provide real-time algorithm processing with them. This report documents the work performed under this contract.

2. Statement of Work

The Statement of Work from the proposal is as follows:

The contractor shall, unless otherwise specified herein, supply the necessary personnel, facilities, services, and materials to accomplish the following tasks within a one and one-half year period following receipt of funding.

1. Upgrade the hardware and software design of the Day/Night WSI system to enable a 500' separation between the user and the sensor.

2. Provide two automated Day/Night Whole Sky Imagers for detection of day and night sky fields. These systems will include the design upgrade from item 1 and also include the capability to acquire NIR digital images.

3. Provide a set of 250' cables for the existing Day/Night WSI.

Under the optional budget, if funded, the contractor shall accomplish the following within a two year period.

4. Coordinate with the sponsor regarding the most appropriate tasks and estimated costs for further development.

5. Provide personnel trained in the WSI and its capabilities to address these tasks to the limit of funding provided under the optional budget. These tasks may include analysis, software development, documentation, minor hardware development, and other tasks related to the WSI which are mutually agreed by the sponsor and by MPL to be appropriate.

The budget for Part 1 was $720,000, and the budget for Part 2 was $195,754. The initial funding was received about June 99. The tasks for Part 1 were all completed by about Oct 00. Item 1, to redesign the system for a 500' separation, will be discussed in Section 3. The two new WSI units 13 and 14 were completed by about Oct '00. Unit 14 was delivered to the sponsor in N. California on 5 Oct 00, and Unit 13 remained at MPL under test. Units 13 and 14 are discussed in Section 3. Task 3 of Part 1 was to deliver a 250' cable set for Unit 12, the previously existing D/N WSI. This was delivered 22 Sep 99.

The work under the options was also funded. In addition, a follow-on contract, N00014-01-D-0043 DO #4 was partially funded at the same time that the options were funded. The agreed-upon work completed under these options and under the start of the follow-on contract may be summarized as follows.

1. Develop a first version night algorithm, and implement it in the field.

2. Derive the geometric calibrations and other inputs as necessary to put night algorithms into place.

3. Modify the Day cloud algorithm to include a horizon mask and an occultor mask. Write code to extract the daytime clear sky background ratio, and extract the clear sky background library for use with the Day algorithm.

4. Upgrade D/N WSI Unit 12 for real-time processing.

5. Modify the Unit 13 and 14 processing code interface to handle the case when the sponsor's computer is not operational.

All of this work under the options was completed. The night algorithm was written, and the geometric calibrations and other inputs completed prior to Oct '00. The first night algorithm was fielded in Oct '00 on Unit 14, and in Jan '01 on Unit 12 at SOR. It was further improved and installed on Unit 12 in Feb '01. It has been in use on Unit 12 since that time. It was programmed into the processing code for Units 13 and 14, however it was never fully implemented on these two units due to changes in sponsor priorities. The night algorithm is discussed in Section 7.

The day algorithm was updated, and the new clear sky background provided, in Feb '01. This work is discussed in Section 6. Unit 12 was updated in Jan '01, to include real-time processing and the NIR filter. This work is discussed in Sections 4 and 5. The Unit 13 and 14 computer interface was modified and documented in Memo AV01-030t.

Following this time, work was slowed on the project, in order to retain most of the remaining funds for an eventual deployment of Unit 13. Unit 13 was never deployed due to changing sponsor requirements (caused by changing national priorities following 9/11), however it continued to run well at MPL. In addition, we processed all of the radiometric calibrations for all three units. In July '01, Unit 14 was returned to MPL at the close of the deployment, and a few upgrades were made. During the remainder of the contract period, work was done to support the sponsor's interest in several general areas, including working on beam transmittance distribution, documenting the algorithms, software test, and general site support. All work was completed by May '03.

3. New Day/Night WSI Design and Fabrication (Units 13 and 14)

The primary goal of the WSI re-design was to enable having the WSI at least 500' from the user. It is perhaps appropriate to include an overview of the D/N WSI before discussing this upgrade. The D/N WSI is designed to acquire imagery 24 hours a day, 7 days a week, for detection of cloud fields as well as sky radiance distribution if desired. It is fully automated, and environmentally hardened. Its primary components include a fisheye lens, spectral and neutral density filter wheels, and a 16 bit cooled CCD sensor. A solar/lunar occultor shades the lens and dome, to minimize stray light contamination.

The D/N WSI Unit12 is shown in Figure 1. A typical daytime image is shown in Figure 2, and a moonlight image in Figure 3. A more detailed discussion of the WSI with more imagery may be found in Shields et al 2003a, shown in Attachment 1.

In order to separate the user by 500' from the sensor, we were concerned that the present design would cause problems. Specifically, the camera manufacturer was not confident that the camera cable would work over that length, and the simple weight of the remaining cables would become unwieldy. Thus we decided to integrate the controller (often referred to as the "blue box") into the sensor environmental housing. This required integrating the control computer, the electronics Accessory Control Panels (ACP), and a monitor into the environmental housing. The resulting design is shown in Figure 4.

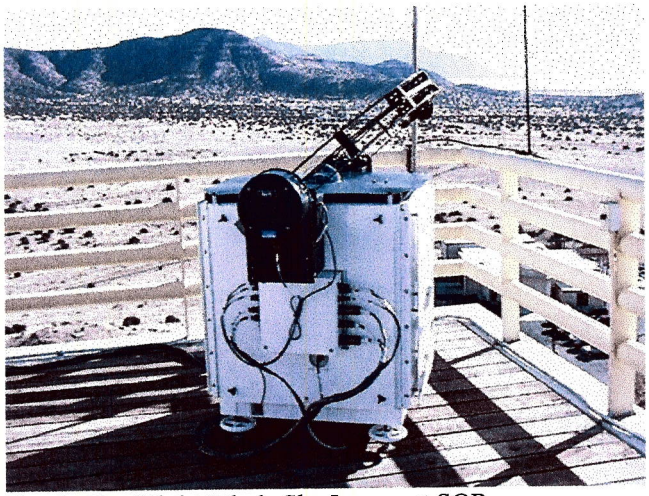

Fig. 1. Day/Night Whole Sky Imager at SOR

Fig. 2. Daytime Image

Fig. 3. Moonlight Cirrus

Fig. 4 New design with controller in environmental housing

The system uses an environmentally hardened control computer mounted on the side of the sensor housing. The two ACP's (sensor and occultor) were redesigned to go into a single ACP unit on a single board, and to use more readily available electronic components. (The original ACP design was over 10 years old, and some of the components were starting to be unavailable.) As a result of this change, the controller used on the older systems such as Unit 12 is not longer required, and the heavy cable bundle connecting the sensor and the controller are not required. Moreover, the sensor is only connected via Ethernet to a processing computer, and separation between the user and the sensor can be at least 500' or longer.

In addition, several improvements were made where feasible. For example, the coolant flow mechanism has been simplified, and the filter changer improved. The camera housing mating has been improved with an o-ring seal between the camera housing and the environmental housing. Several of the subassemblies are shown in Figures 5 a – c, and the new assembly drawing is shown in Figure 5d.

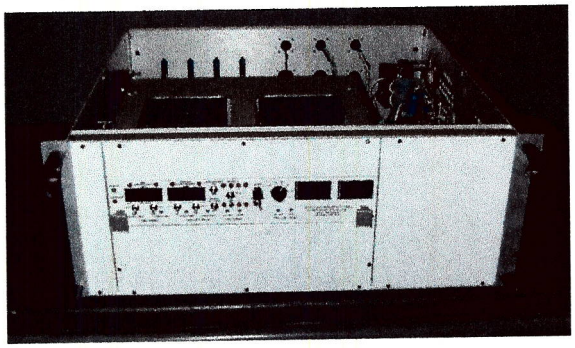

5a) New ACP

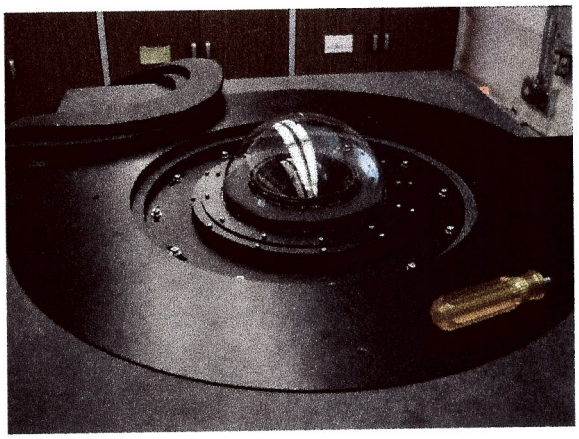

5b) Top of housing

Fig. 5. New assembly components. Fig 4a shows the new single-board ACP. Fig. 4b shows the top of the housing, with the top sheet removed. Fig 4c shows the new configuration inside the housing, and Fig. 4d is the assembly drawing.

5c) Inside housing

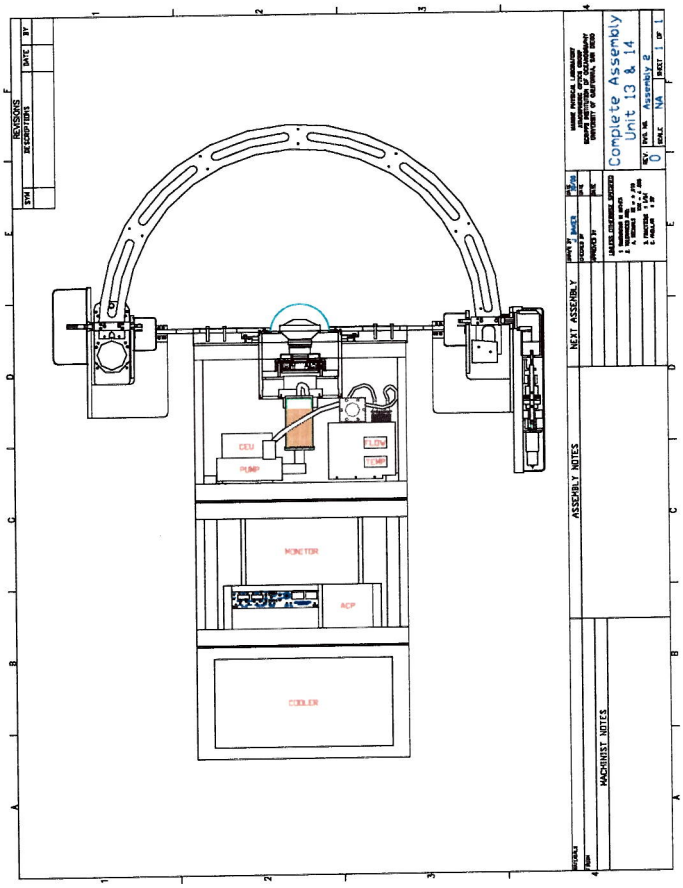

5d) Assembly drawing

Perhaps the most important design change is that a processing computer has been added, to enable near-real time processing of the data to yield cloud decision. Previously, the control computer was able to process to cloud decision during the daytime. In order to enable maximum data acquisition rates, a processing computer was added, for processing both day and night algorithms to yield 24-hour cloud decision results.

In addition, a sophisticated interface with a third computer was added. This computer was intended to be the computer controlling another system, the EPAODMS, provided by another group. The software and interface are further discussed in Section 5.

Both units were fully calibrated radiometrically, so that radiance data would be available for cloud algorithm development work. The calibration memos are listed in the references section. A setup memo with detailed instructions for setup was provided, as well as maintenance instructions. The software, which will be discussed in Section 5, was documented in memos provided to the sponsor.

Unit 14 was delivered to a site in Northern California in Oct'00. It was returned to MPL several months later due to changes in sponsor priorities (resulting from changes in national priorities following 9/11). Units 13 and 14 operated almost flawlessly at MPL for an extended period. Unit 14 is now deployed at another site for one of SOR's programs.

4. Hardware Modifications to Unit 12

The D/N WSI Unit 12 at SOR was delivered under another contract, in January '99. In comparison with Unit 2, the last D/N WSI fielded at SOR, several major changes had been made. (These updates also all applied to the subsequent Units 13 and 14.)

a) The housing is a much stronger metal housing appropriate for more demanding environmental conditions.
b) Several sensors were added to monitor the internal conditions, such as the coolant flow, and enable the camera to be automatically turned off if it was at risk.
c) A much stronger occultor mechanism using a pair of arcs that move from East to West and a trolley that moves from North to South.
In comparison with Units 3 – 11, the following upgrades had been made.
a) The camera hardware was upgraded to a Series 300 camera.
b) The computer hardware and software were upgraded to run under Windows 95.
c) A new solar occultor trolley mechanism was developed that was much more reliable. It uses a single chain drive, and incorporates a slip clutch, as well as several other new features
d) The cabling was modified to enter the sensor's environmental housing via a junction box, which is a cleaner package mechanically and electrically.
e) The Daytime cloud algorithm was added to the control computer.

Under this contract, modifications were made to bring Unit 12 up to the standards of Unit 13 and 14, as much as feasible without major hardware costs. The controller was not

integrated into the sensor system, however a processing computer was added to the system, to enable running the processing program in real time. Although it was previously possible to run the day cloud algorithm between image grabs, this slowed the acquisition rate. By moving the algorithm onto a second computer, this enabled acquisition at every minute during the day and every two minutes at night. New versions of the control code and the processing code that are very similar to the Unit 13 and 14 processing code, were added to the system. A Near Infrared (NIR) filter was installed and added to the data collection sequence.

As discussed in Sections 6 and 7, the day algorithm was updated with a new background sky library, and the algorithm was adjusted for the sky conditions at SOR. The new night algorithm was installed and fully enabled, with several upgrades over the next few months. As a result of this development, Unit 12 was operating and providing cloud decision results on a 24-7 basis. The Unit 12 hardware upgrade is documented in Memo AV01-031t.

5. Software Modifications

The software for both the Unit 12 and the Unit 13/14 configurations have been significantly changed and updated under this contract. For both of these configurations (12 vs. 13/14), the control computer program RunWSI is designed to enable the WSI to acquire data at user-selected intervals, such as every 2 minutes or 10 minutes. Images are acquired in the Blue, Red, and NIR during the daytime, and open hole at night. The program drives the solar/lunar occultor, on the basis of the time and location (determined from GPS or internal clock). The occultor is driven to the sun, if it is out, or else to the moon or the Eastern horizon if there is no moon.

The flux control algorithm determines the proper selection of neutral density filter and exposure time, using the time of day and associated solar zenith angle, lunar zenith angle, lunar phase angle, and lunar earth-to-space distance. The program also controls the filter changer and the camera.

The program monitors the system health, by recording camera chip temperature, camera housing temperature, environmental housing temperature, coolant flow rate, and pressure of the nitrogen gas used to purge the camera housing. Yellow flags, indicating an alert, and red flags, indicating potential risk to the instrument or data quality, are sent to the user and recorded on the image headers. In the event of potentially damaging conditions, such as temperatures that are out of range, the camera is automatically turned off by the program, and then turned back on when satisfactory conditions resume.

Data are sent to the processing computer, where they are processed to yield cloud decision images, and the raw and processed data may be archived. Normally, the data are transferred to a third computer for archival.

The primary difference between the two systems is that Unit 12 uses the older design with a separate controller, as illustrated in Fig. 6, and the controller has been integrated

into the environmental housing for Units 13 and 14, as shown in Fig. 7. Figure 6 shows four elements: a sensor, a controller computer, a processing computer, and a user system. In Figure 7, the sensor and controller computer have been combined into one package, so there are only three elements: a sensor with controller, a processing computer, and a user system. Both WSI systems are able to process data in near-real time, and communicate with an external system, to provide cloud decision results and cloud fractions for the sky and selected regions of interest.

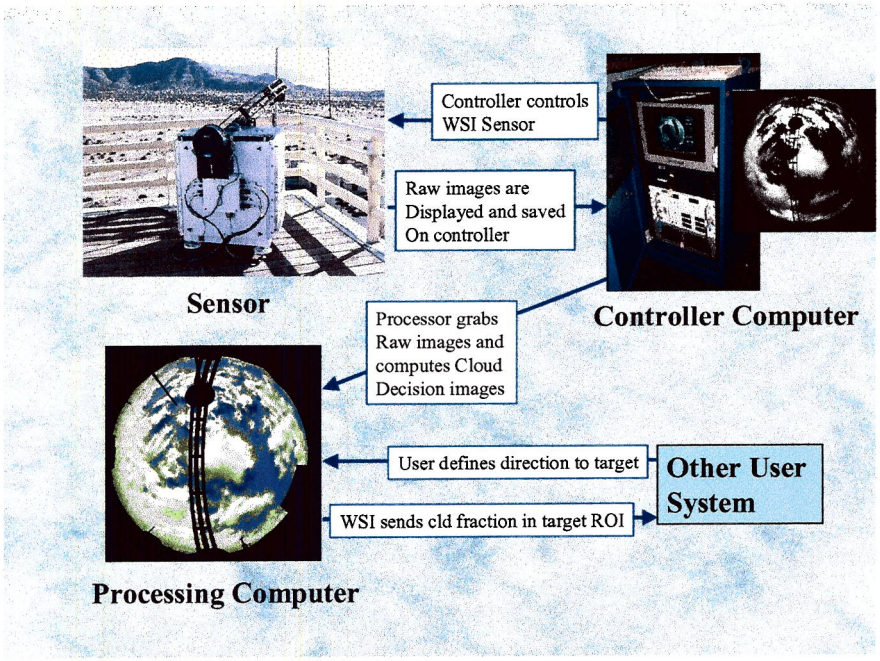

Fig. 6 Configuration for Unit 12, with separate controller

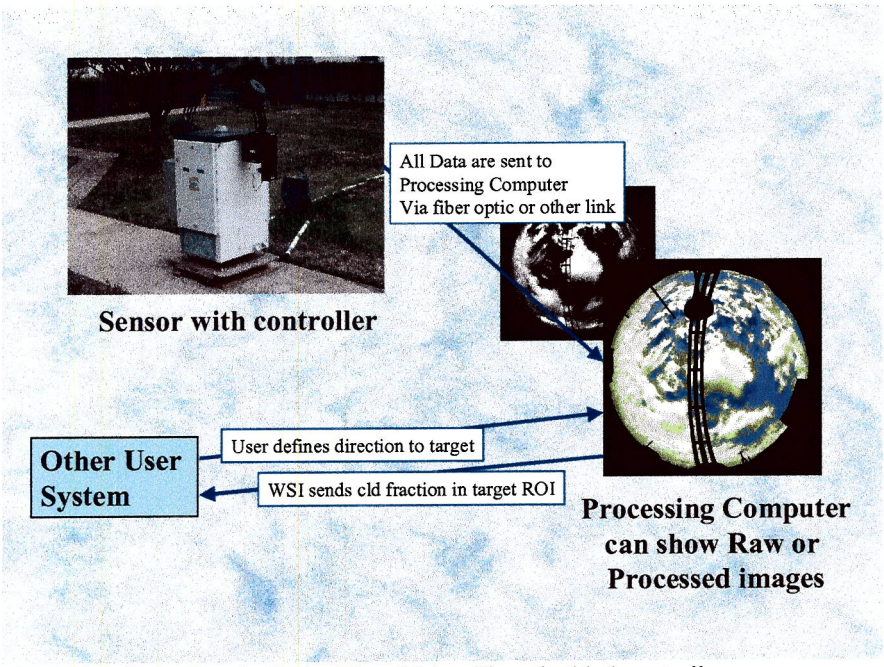

Fig. 7 Configuration for Units 13 and 14, with embedded controller

The other primary difference between the systems is that the Unit 12 control computer operates with Windows 95, and its control program is a Windows program written in C. The Unit 13/14 control computers operate with Windows NT, and the control program is an extensive "script" written for the V++ program. V++ is an image acquisition and processing development environment provided by the camera manufacturer. The Unit 12 processing computer is running under Windows NT, and the program is a Windows program written in C. The Unit 13 and 14 processing computer is also running under Windows NT, but its program is slightly more sophisticated in terms of its handling of headers and other details. (It was not practical to modify the Unit 12 code for the same sophistication.) We do not recommend using V++ in the future, as it has taken a significant time investment to the make the software reliable and avoid system hangs due to limitations of V++.

The details of the software modifications are discussed in the memos. Memos AV00-035t and 036t document the control and processing programs initially installed with Units 13 and 14. Memo AV01-029t provides an overview of the changes to the Unit 12 software. Memo AV01-030t documents upgrades to the Unit 13/14 software. Memo AV01-033t provides an overview of the history of the upgrades to unit 12 control software, including one upgrade made after Memo AV01-029t was written. Memo AV01-034t documents the upgrades to the Unit 12 processing software made after Memo AV01-029t was written. The algorithm upgrades inherent in this code will be discussed in Sections 6 and 7.

6. The Day Algorithm

The day cloud algorithm is discussed in the attached paper. The algorithm depends on the use of a clear sky background library. Up until this time, we had not written programs to enable extracting the clear sky background for these images, and we had been using the clear sky background extracted from another instrument. Memo AV01-032t documents the new programs and procedures, and Memo AV01-035t documents the data used to pull the library. As part of this process, we also optimized all the other inputs for the calibration.

Since this time, we have developed a new algorithm based in part on the NIR/blue ratios, and in part on the spatial texture in the image. This new algorithm has been developed for a Day WSI system, with a different camera format, so it would need to be converted to run with the D/N WSI, but we highly recommend integrating this new algorithm into the D/N WSI code. The new algorithm uses the NIR images, where there is a higher contrast between the thin clouds and the background. It also uses the spatial texture in the image to adjust each image for varying haze amount. The sunrise and sunset handling is also improved, although not yet optimized.

7. The Night Algorithm

In tests made in the early 90's, we found that the daylight algorithm worked well for at least some moonlight cases. However we had not developed a starlight algorithm, nor

had the moonlight algorithm been automated. At the time this project was funded, the concepts for a first generation starlight algorithm had been developed under funding from another sponsor. This work is documented in Shields et al, 2002 and Tech Memo AV99-044t. This algorithm had not yet been converted to work in the field, and it was quite preliminary. Under this contract, the starlight algorithm was further developed, to cover both starlight and moonlight, and it was converted for use in the field. It was included in the processing code on Units 13 and 14 in Sep 00. The night algorithm was improved considerably prior to delivery for Unit 12 in Jan 01. Additional upgrades were provided in Feb 01. The Unit 13 and 14 processing code is documented in Memo AV00-036t, the Unit 12 processing code is documented in Memo AV01-029t, and the updates are documented in Memo AV01-034t. (The night code is not mentioned in the first two memos, but the third memo documents that it was present in all three versions of the code.) The logic used in the final version, which is still fielded on Unit 12, is documented in Memo AV03-30t.

The starlight algorithm was installed but not activated on Units 13 and 14, due to changes in sponsor priorities. However, the algorithm has been running routinely on the Unit 12 sensor at SOR. Our sponsors tell us that it performs reasonably well. The rest of this section provides a brief overview of the algorithm logic. For more details, see memos AV99-044t and AV03-030t. We will also discuss more recent upgrades to the assessment of the sky condition, and concepts for full resolution night algorithms.

The current night algorithm fielded on Unit 12 at SOR is based on detection of stars. The star library from the National Space Science Data Center (Hoffleit 1991) provides information including right ascension, declination, and magnitude for over 9100 stars, down to magnitude 8. Software was written to convert these angles to zenith angle θ and azimuth angle φ with respect to a known location. A geometric calibration accurate to approximately half a pixel is used to map θ, φ positions into x, y positions on the image.

The next step is to search for a star in the predicted location. The program finds the largest pixel value within a two-pixel radius of the predicted location. We have found that the point spread function of the star is reasonably modeled by a Gaussian curve with a width (STD) of 0.45 pixel. Using a Levenberg-Marquardt best fit routine, the program attempts to fit a two-dimensional Gaussian curve to the data (and in the process determines the true pixel-center of the peak in image space). If the fitting routine gives a reasonable result, the program counts this as a successful detection of the star in the image.

Using this technique, we were able to detect most of the stars from magnitude 1 to magnitude 7 in a sample clear image. For example, for zenith angles 30 degrees or less, the program detected 100% of the 33 stars of magnitude 0 to 4, and 88% of the 99 stars of magnitude 0 to 7. For zenith angles of 70 degrees or less, the program detected 78% of the stars of magnitude 0 to 7. The algorithm automatically rejected many of the undetected stars, because it rejects any stars that are near other stars. A test of random locations in an overcast image resulted in a 5% false detection rate.

The version of the algorithm fielded in Sep '00 used stars up to magnitude 6 stars under starlight, yielding about 5000 stars total, and about 2100 stars in a typical image. Under moonlight, only up to magnitude 5, for 800 stars, was used. A number of criteria were used to identify a successful detection, such as error in the fit. The contrast between the area under the Gaussian and the background was computed. Opaque clouds were identified using a fixed contrast threshold, and thin clouds were identified using a contrast threshold depending on zenith angle and star magnitude.

Each star resulted in a cloud free, thin or opaque estimate for that specific star. The sky is then divided into 356 cells, typically 5 degrees in zenith by 15 degrees in azimuth, as shown in Fig. 8. In each cell, the fraction of successful detections are counted. Cells with less than 50% of stars detected are called "no cloud", and other cells are called "cloud". Cloud cells with more "opaque" than "thin" detections are called opaque. All pixels within a cell are identified in the same category.

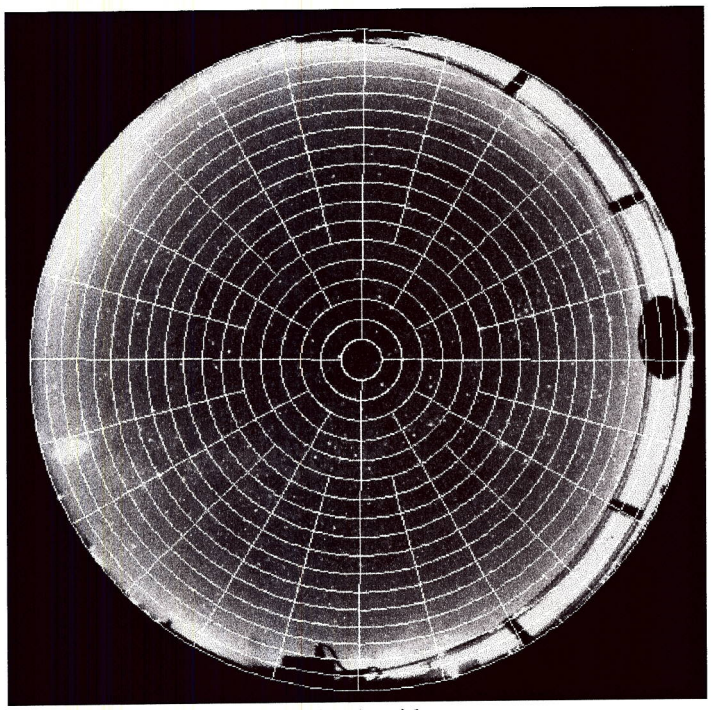

Fig. 8. Sky cells used for night algorithm

The version of the algorithm used in the field also masks out any parts of the image that are not valid sky data, such as areas blocked by the occultor. Data are dark-corrected, but are not otherwise calibrated in this version of the program. The appropriate contrast threshold for the zenith was found to vary with both star magnitude and moon condition, as shown in Fig. 9. A discussion of further details is given in Memo AV03-030t, which is included as Appendix A.

The results were reasonably good for the test cases we had available. One example is shown in Fig. 10, and additional examples are given in the Appendix. In Fig. 10, blue is identified as clear, yellow as thin cloud, white or grey as opaque cloud, and black as no

data. The bright region near the left side of the image is due to the lights of Albuquerque. The algorithm clearly does not handle this region. The results are quite good for the rest of the image however.

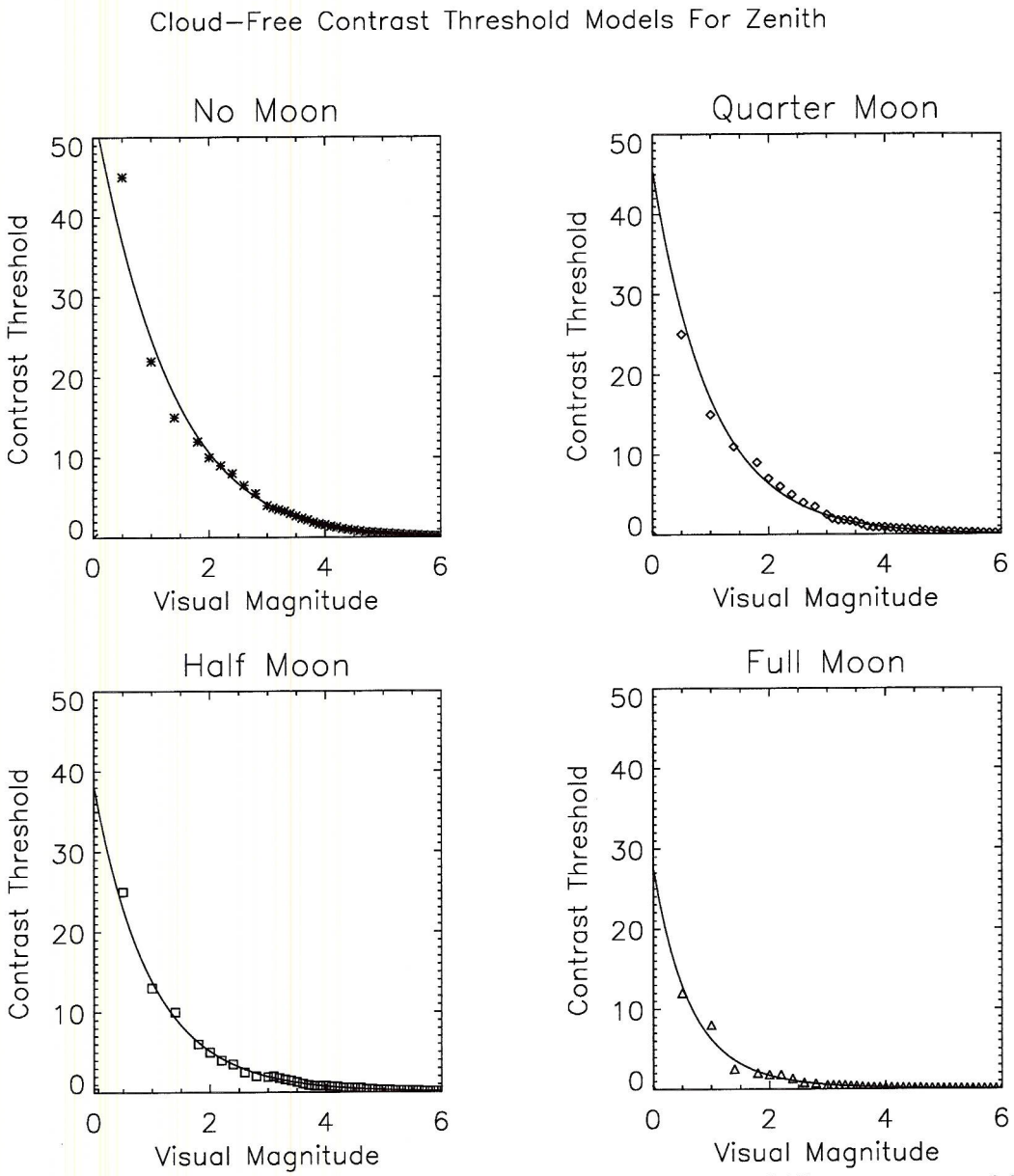

Figure 9. Star contrast at zenith point as a function of star magnitude. Solid lines represent model of data.

We hope to soon have the opportunity to evaluate the results of the cloud night algorithm for many nights, in order to better assess its effectiveness. It should be noted that if the camera is bumped hard enough to change the alignment by a few pixels, the geometric calibration needs to be re-generated, and the night algorithm may not be effective until this new calibration is completed. The geometric calibration can be completed from the starlight imagery on a clear night. In the future, it may be worth considering adding an inexpensive impact detector, such as used on shipping crates, to enable the user to know when the system may be out of alignment.

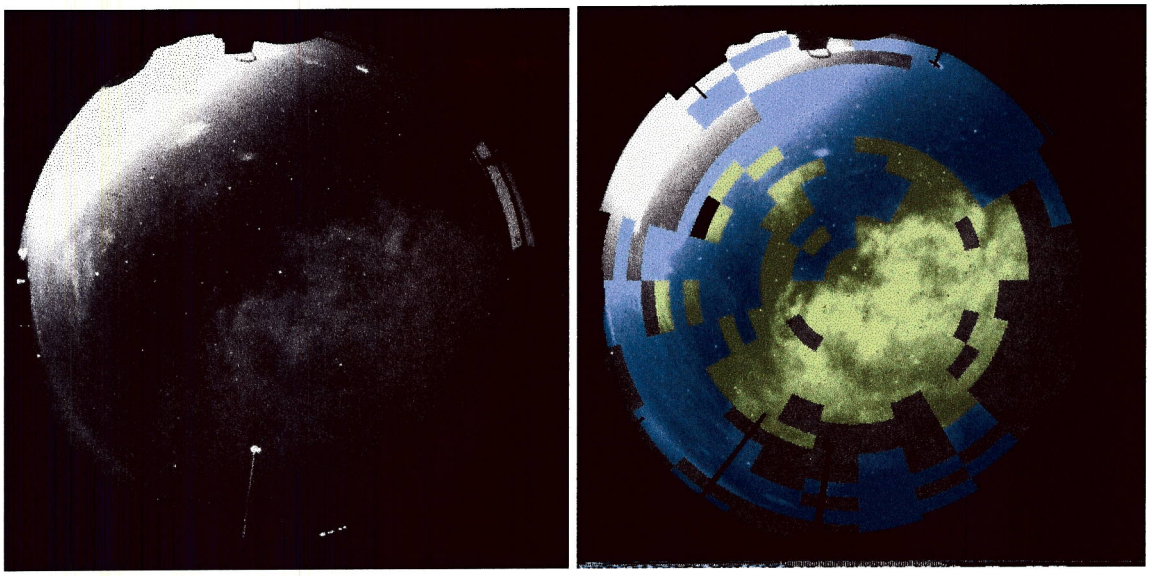

Fig. 10 Sample raw image and cloud decision image for night sky scattered-cloud case

Before leaving the subject of the night algorithm, we would like to note two additional developments. First, under another contract, significant work has been done to work with the absolute radiance images in order to extract the earth-to-space beam transmittance distribution. This is discussed in Shields et al 2004, and an example of the results is shown in Fig. 11. We feel that this work can be the basis of a more accurate night cloud algorithm. Secondly, a method for extending the night algorithm to provide full resolution data has been conceptualized, and may be developed under future contracts. This would enable cloud determination at the full pixel resolution level used in the Day algorithm.

In summary, the current night algorithm is based on detection of stars within each of 357 cells. The stars are detected from the shape of the point-spread function, represented by a Gaussian curve of width 0.45 pixel. The contrast is determined from the area under the Gaussian, and the background level. The determination of the presence of opaque of thin cloud in the direction of the star is based on a contrast threshold that depends on star magnitude, moon phase and look angle.

8. Summary

The capabilities of the Day/Night WSI systems took a major step forward under this contract. The design was upgraded in several respects, and the system control was integrated into the housing so that the only cables required to go into the system are the power cables and the Ethernet link. This enables the system to be fielded at large distances from the user. Processing computers were added, to extract the raw data and generate cloud decision images in near-real time. The processing computers also can communicate with an additional computer, to provide results and images for the whole sky or regions of interest selected by the third computer.

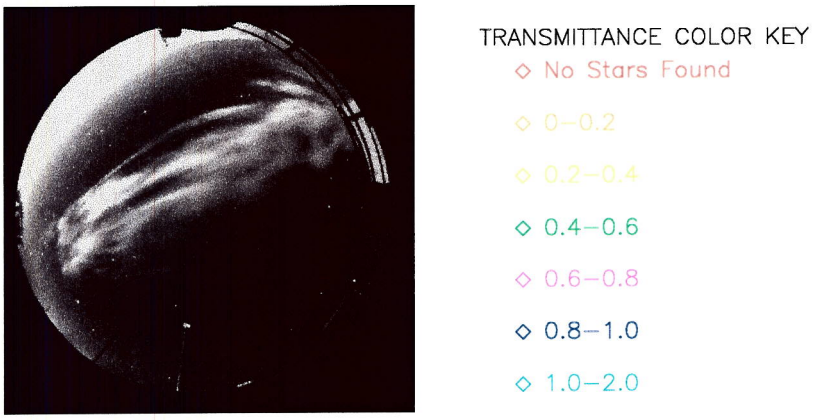

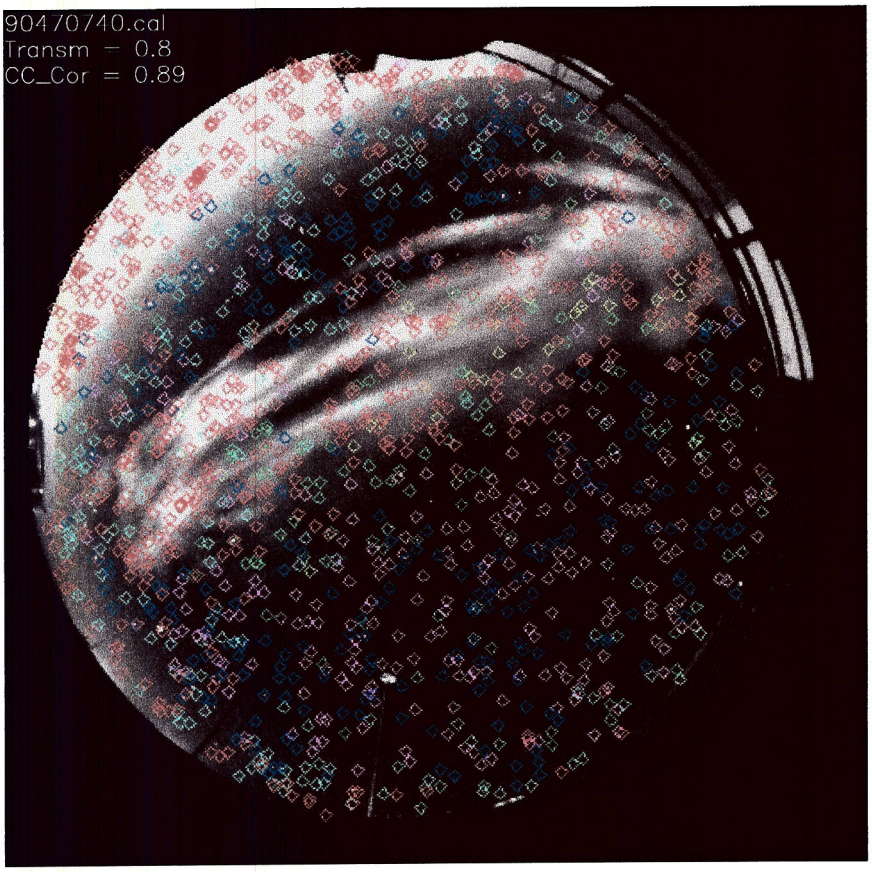

Fig. 11. Transmittance map for thin cloud image, 0.8 aerosol correction applied, calibration correction of 0.89 applied.

Day algorithms were updated, and the sky background for the Unit 12 camera and location were installed. A new night algorithm was developed and fielded. Our sponsors have been very pleased with the operation of the instruments. We are told that the algorithm operates quite well in the daytime, and reasonably well at night.

There was only limited funding under these contracts for the algorithm upgrades, and much of the funds were used to develop and field the instruments. In spite of this, we are

pleased with the initial performance of the algorithms. As discussed in the text, we have also developed concepts for major additions to both day and night algorithms in the future.

9. Acknowledgements

We would like to express our appreciation to the personnel of Starfire Optical Range and their contractors from Boeing. Dr. Robert Fugate, the head of SOR, Ann Slavin, our acting contract monitor, and Steve Fisher, who has interfaced with us on hardware, have all been a pleasure to work with, as has Capt. Jon Saul, who has interfaced with us on hardware more recently. We especially appreciate the work of Ann Slavin in her role in monitoring our work. This project is always a pleasure to work on, due to the technical capability and understanding, and cooperative working attitude of our sponsors. Our thanks to the Air Force and the Starfire Optical Range for funding this work.

10. References

In-house Technical Memorandums available at sponsor's request

Burden, A. R. and J. E. Shields, "Preliminary Results of Starlight-Based WSI Cloud Algorithm", Atmospheric Optics Group Technical Memorandum AV99-044t, 17 Aug 99.

Shields, J. E., "Setup Instructions for WSI Field Units 13 and 14", Atmospheric Optics Group Technical Memorandum AV00-034t-mod, 14 Aug 00, mod 20 Oct 00.

Karr, M. E., "Control Computer operations overview for WSI units 13 and 14", Atmospheric Optics Group Technical Memorandum AV00-035t, 15 Sep 00.

Karr, M. E., "Processing Computer operations overview for WSI units 13 and 14", Atmospheric Optics Group Technical Memorandum AV00-036t, 15 Sep 00.

Shields, J. E., "Unit 14 Parts List", Atmospheric Optics Group Technical Memorandum AV00-038t, 20 Oct 00.

Shields, J. E., "Occultor and WSI Controller Calibration for Units 13 and 14", Atmospheric Optics Group Technical Memorandum AV01-024t, 16 Jan 01.

Karr, M. E., "Unit 12 Software Updates", Atmospheric Optics Group Technical Memorandum AV01-029t, 29 Jan 01.

Karr, M. E., "Update to ProcWSI for Units 13/14", Atmospheric Optics Group Technical Memorandum AV01-030t, 29 Jan 01.

Shields, J. E., "SOR Trip Report, Jan '01 (Upgrade of Unit 12)", Atmospheric Optics Group Technical Memorandum AV01-031t, 28 Feb 01.

Shields, J. E., "Procedure for Processing SOR Cloud Library Data", Atmospheric Optics Group Technical Memorandum AV01-032t, 28 Feb 01.
Karr, M. E., "SOR RunWSI Updates", Atmospheric Optics Group Technical Memorandum AV01-033t, 28 Feb 01.

Karr, M. E., "SOR ProcWSI Updates", Atmospheric Optics Group Technical Memorandum AV01-034t, 28 Feb 01.

Shields, J. E., "SOR Clear Sky Background Library File Generation for Unit 12", Atmospheric Optics Group Technical Memorandum AV01-035t, 6 Apr 01.

Burden, A. R., "Basic Geometric Calibration of WSI Unit 12", Atmospheric Optics Group Technical Memorandum AV01-041t, 10 Jun 01.

Burden, A. R., "Unit 12 Rolloff Calibration", Atmospheric Optics Group Technical Memorandum AV01-042t, 18 Jun 01.

Burden, A. R., "Unit 12 Flat Field Calibration", Atmospheric Optics Group Technical Memorandum AV01-043t, 23 Jun 01.

Burden, A. R., "Unit 12 Linearity and Exposure Calibration Results", Atmospheric Optics Group Technical Memorandum AV01-044t, 23 Jun 01.

Burden, A. R., "Unit 12 Effective Lamp Irradiance Computation", Atmospheric Optics Group Technical Memorandum AV01-045t, 20 Jun 01.

Burden, A. R., "Unit 12 Aperture Calibrations", Atmospheric Optics Group Technical Memorandum AV01-046t, 22 Jun 01.

Burden, A. R., "Absolute Calibration Results for Unit 12", Atmospheric Optics Group Technical Memorandum AV01-047t, 20 Jun 01.

Burden, A. R., "Unit 12 Calibration Summary", Atmospheric Optics Group Technical Memorandum AV01-048t, 27 Jun 01.

Burden, A. R., "Basic Geometric Calibration of WSI Unit 13", Atmospheric Optics Group Technical Memorandum AV01-049t, 10 Jun 01.

Burden, A. R., "Unit 13 Rolloff Calibration", Atmospheric Optics Group Technical Memorandum AV01-050t, 28 Jun 01.

Burden, A. R., "Unit 13 Flat Field Calibration", Atmospheric Optics Group Technical Memorandum AV01-051t, 27 Jun 01.

Burden, A. R., "Unit 13 Linearity and Exposure Calibration Results", Atmospheric Optics Group Technical Memorandum AV01-052t, 26 Jun 01.

Burden, A. R., "Unit 13 Effective Lamp Irradiance Computation", Atmospheric Optics Group Technical Memorandum AV01-053t, 22 Jun 01.

Burden, A. R., "Unit 13 Aperture Calibrations", Atmospheric Optics Group Technical Memorandum AV01-054t, 26 Jun 01.

Burden, A. R., "Unit 13 Acrylic Dome Calibration", Atmospheric Optics Group Technical Memorandum AV01-055t, 26 Jun 01.

Burden, A. R., "Absolute Calibration Results for Unit 13", Atmospheric Optics Group Technical Memorandum AV01-056t, 26 Jun 01.

Burden, A. R., "Unit 13 Calibration Summary", Atmospheric Optics Group Technical Memorandum AV01-057t, 29 Jun 01.

Burden, A. R., "Basic Geometric Calibration of WSI Unit 12", Atmospheric Optics Group Technical Memorandum AV01-041t, 10 Jun 01.xx

Burden, A. R., "Basic Geometric Calibration of WSI Unit 14", Atmospheric Optics Group Technical Memorandum AV01-058t, 10 Jun 01.

Burden, A. R., "Unit 14 Rolloff Calibration", Atmospheric Optics Group Technical Memorandum AV01-059t, 29 Jun 01.

Burden, A. R., "Unit 14 Flat Field Calibration", Atmospheric Optics Group Technical Memorandum AV01-060t, 27 Jun 01.

Burden, A. R., "Unit 14 Linearity and Exposure Calibration Results", Atmospheric Optics Group Technical Memorandum AV01-061t, 27 Jun 01.

Burden, A. R., "Unit 14 Effective Lamp Irradiance Computation", Atmospheric Optics Group Technical Memorandum AV01-062t, 27 Jun 01.

Burden, A. R., "Unit 14 Aperture Calibrations", Atmospheric Optics Group Technical Memorandum AV01-063t, 27 Jun 01.

Burden, A. R., "Unit 14 Acrylic Dome Calibration", Atmospheric Optics Group Technical Memorandum AV01-064t, 27 Jun 01.

Burden, A. R., "Absolute Calibration Results for Unit 14", Atmospheric Optics Group Technical Memorandum AV01-065t, 27 Jun 01.

Burden, A. R., "Unit 14 Calibration Summary", Atmospheric Optics Group Technical Memorandum AV01-066t, 29 Jun 01.

Shields, J. E., "Return of SOR Unit 14 from Northern California, 3 July 01", Atmospheric Optics Group Technical Memorandum AV01-070t, 10 Jul 01.

Shields, J. E., "Unit 13 Parts List", Atmospheric Optics Group Technical Memorandum AV01-080t, 6 Sep 01.

Burden, A. R., "Improvements Made to Starlight-Based Cloud Algorithm", Atmospheric Optics Group Technical Memorandum AV03-030t, 19 May 03.

General References

Johnson, R. W., W. S. Hering and J. E. Shields (1989), "Automated Visibility and Cloud Cover Measurements with a Solid-State Imaging System", Marine Physical Laboratory, Scripps Institution of Oceanography, University of California San Diego, SIO 89-7, GL-TR-89-0061, NTIS No. ADA216906

Johnson, R. W., J. E. Shields, and T. L. Koehler (1991), "Analysis and Interpretation of Simultaneous Multi-Station Whole Sky Imagery", Marine Physical Laboratory, Scripps Institution of Oceanography, University of California San Diego, SIO 91-3, PL-TR-91-2214

Shields, J. E., R. W. Johnson, and T. L. Koehler, (1993), "Automated Whole Sky Imaging Systems for Cloud Field Assessment", Fourth Symposium on Global Change Studies, 17 – 22 January 1993, American Meteorological Society, Boston, MA

Shields, J. E., R. W. Johnson, and M. E. Karr, (1994), "Upgrading the Day/Night Whole Sky Imager from Manual/Interactive to Full Automatic Control", Marine Physical Laboratory, Scripps Institution of Oceanography, University of California San Diego, Report MPL-U-140/94

Shields, J. E., R. W. Johnson, M. E. Karr, and J. L. Wertz, (1998), "Automated Day/Night Whole Sky Imagers for Filed Assessment of Cloud Cover Distributions and Radiance Distributions", Tenth Symposium on Meteorological Observations and Instrumentation, 11 – 16 January 1998, American Meteorological Society, Boston, MA

J. E. Shields, M. E. Karr, A. R. Burden, R. W. Johnson and J. G. Baker, (2002) "Analytic Support of the Phillips Lab Whole Sky Imager, 1997 - 2001", Final Report for Contract N00014-97-D-0385. Also issued as Marine Physical Lab, Scripps Institution of Oceanography, University of California San Diego, Technical No. 257.

J. E. Shields, R. W. Johnson, M. E. Karr, A. R. Burden, and J. G. Baker, (2003a) "Whole Sky Imagers for Real-time Cloud Assessment, Cloud Free Line of Sight Determinations and Potential Tactical Applications", The Battlespace Atmospheric and Cloud Impacts on Military Operations (BACIMO) Conference, 2003. Also issued as Marine Physical Lab, Scripps Institution of Oceanography, University of California San Diego, Technical Note No. 261.

Shields, J. E., M. E. Karr, A. R. Burden, R. W. Johnson and J. G. Baker, (2003b), "Analysis and Measurement of Cloud Free Line of Sight and Related Cloud Statistical Behavior", Final Report for Contract N00014-97-D-350 DO #2. Also issued as Marine Physical Lab, Scripps Institution of Oceanography, University of California San Diego, Technical No. 262.

Shields, J. E., M. E. Karr, A. R. Burden, R. W. Johnson and J. G. Baker, (2004), "Development of Techniques for Determination of Nighttime Atmospheric Beam Transmittance and Related Analytic Support for the Whole Sky Imager", Final Report for Contract N00014-01-D-043 DO #5, publication in process. Also to be issued as Marine Physical Lab, Scripps Institution of Oceanography, University of California San Diego, Technical No.263.

11. Attachments

Attachment 1, Shields et al 2003a, "Whole Sky Imagers for Real-time Cloud Assessment, Cloud Free Line of Sight Determinations and Potential Tactical Applications", and Attachment 2, Memo AV03-030t "Improvements Made to Starlight-Based Cloud Algorithm", are stored as separate electronic files, and are copied next in the hard-copy version of this report.

Whole Sky Imagers For Real-Time Cloud Assessment, Cloud Free Line of Sight Determinations and Potential Tactical Applications

Janet E. Shields*, Richard W. Johnson, Monette E. Karr, Art R. Burden, and Justin G. Baker
Marine Physical Lab, Scripps Institution of Oceanography, University of California San Diego,
9500 Gilman Dr., La Jolla CA 92093-0701

ABSTRACT

Whole Sky Imagers (WSI) have been developed at the Marine Physical Lab for several military and research applications over many years. This paper discusses several systems useful for real-time monitoring of cloud conditions and radiance distribution, and for tactical applications. We include a discussion of several data products, including the results of a Cloud Free Line of Sight (CFLOS) statistical study based on an evaluation of approximately 800,000 WSI images.

The Day/Night WSI is the most capable of the WSI systems. It can be remotely sited from a user, and can provide near-real-time assessment of cloud conditions during the day and at night. While each unit is designed for a specific application, output products can include day and night cloud fraction, cloud condition along selected tracks or in moving regions of interest, and the absolute sky radiance distribution. The ability to extract earth-to-space beam transmittance is in development. At the smaller end of the instrument system scale, a light-weight WSI has been developed for use in an Unmanned Aerial Vehicle, which could be modified for tactical use. Data acquired by earlier versions of the WSI's have now been processed to yield CFLOS statistics. The data were acquired at one-minute intervals for over two years at several sites in the late 1980's. CFLOS statistics as a function of location, cloud fraction, and look angle will be presented, along with persistence results. A new tactical optical system in early development uses one or more fisheye lenses to enable a user to view the full surround, with simultaneous high-resolution views of selected regions of interest within the scene. This concept has a patent pending, and we foresee that these capabilities can be used for now-casting of battlefield environmental conditions.

Key words: Cloud, radiance, tactical imager, now-cast, UAV, visible, NIR, CFLOS, cloud persistence, battlefield, whole sky imager

1. OVERVIEW

Whole Sky Imagers (WSI) are ground-based sensors which are used in military test site support, global climate research, UV research, and other applications. They are designed to provide high quality digital imagery of sky conditions and, when combined with appropriate algorithms, provide assessment of cloud amount and location within the scene, absolute radiance distribution, and related atmospheric parameters. The Marine Physical Lab (MPL) at Scripps Institution of Oceanography has been very active in the development of WSI systems for the last two decades. The first WSI systems the group developed using digital imaging technology were deployed in the early 1980's, and were followed by fully automated systems in the mid to late 1980s (Johnson et al 1989, and Shields et al., 1993). WSI systems capable of full 24-hour autonomous operation for acquisition of day and night sky parameters were fielded in the early 90's, and have continued to evolve in capability (Shields et al 1998).

* jshields@ucsd.edu; phone (858) 534-1769; fax (858) 822-0665

This paper will give an overview of the development of the WSI sensors, and then discuss the Day/Night WSI data products in more detail, emphasizing those areas that are applicable to military requirements. Sample Cloud Free Line of Sight (CFLOS) statistics will be presented, including persistence results and multi-station results. These CFLOS statistics were processed for the Starfire Optical Range using the Day WSI data-base. Finally, we will discuss the developmental Tactical Full Scene Imager (with patent pending) which can be used to provide unique imagery for a number of tactical applications and environmental now-casting applications.

2. DEVELOPMENT OF FISHEYE IMAGING SYSTEMS AT MPL

The original concept for the development of calibrated fisheye imaging systems at MPL evolved out of the group's Atmospheric Optics program, a measurement and modeling program using multiple sensors for monitoring sky radiance, atmospheric scattering coefficient profiles, and other parameters related to vision through the atmosphere (Johnson et al., 1980). Beginning in the early 1980's, the group developed a series of ground-based calibrated fisheye imaging systems known as Whole Sky Imagers (WSI) that used digital imagery and were fully automated. The first automated WSI was conceived as combining the features of the all-sky cameras used in earlier programs, with the scanning radiometer systems that provided measurements of sky radiance distribution. The first WSI systems used digital cameras (sometimes CCD, sometimes Charge Injection Device or CID imagers), with fisheye lenses, optical filter changers, relay optics to provide the proper image size and location, equatorial sun occultors to provide shading for the fisheye lens, and early versions of personal computers for automated control. Figure 1 shows some of this evolution. The film-based all-sky camera in use in a 1963 deployment is shown in Figure 1a, and the automated Day-only WSI developed in the early and mid-1980's based on CID technology is shown in Figure 1b. With the use of very low noise 16 bit CCD cameras and an occultor modified to handle both sun and moon, these systems were further developed into the Day/Night WSI shown in Figure 1c. Some typical images from the Day/Night WSI are shown in Figure 2.

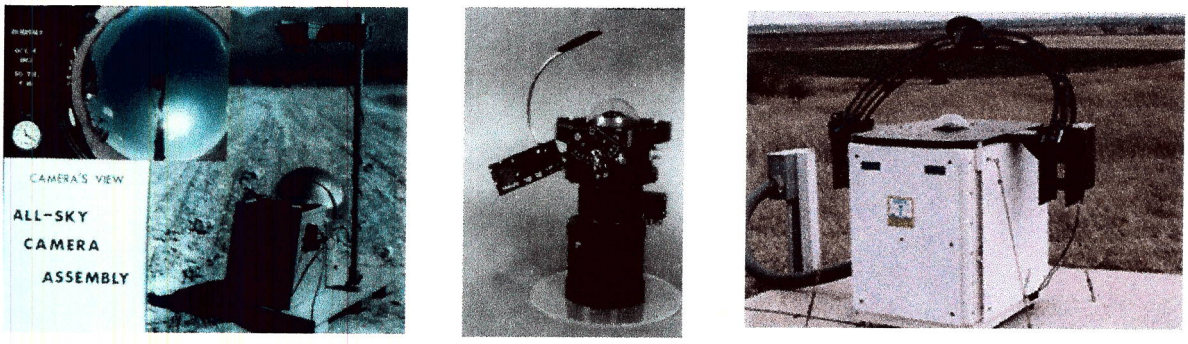

(a) (b) (c)

Figure 1: Some of the WSI Systems developed at MPL that contributed to the development of the Day/Night WSI: a) the All-Sky Camera used in 1963; b) the Day-only WSI used in the 1980's; c) the Day/Night WSI used in 1990's and currently in use.

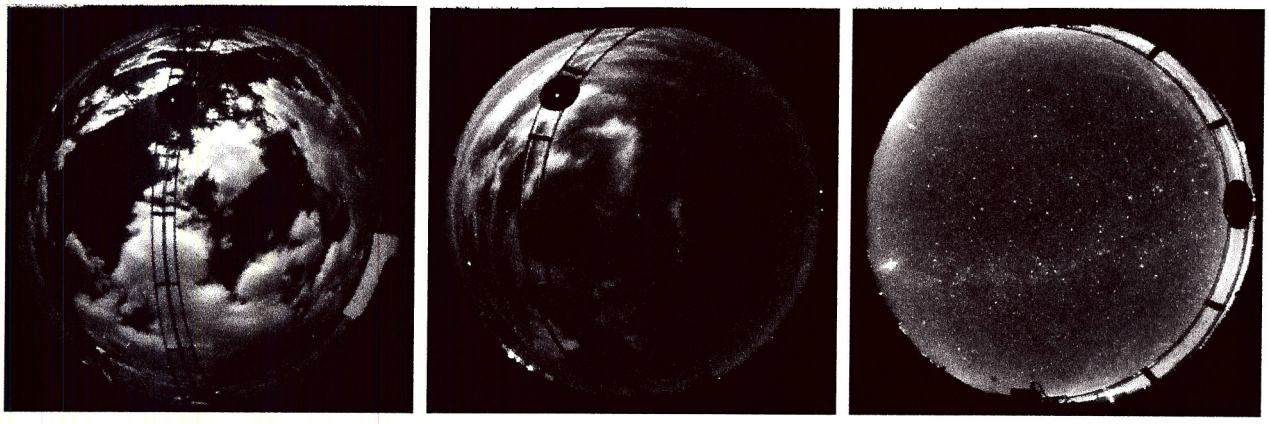

Figure 2: Sample imagery from the Day/Night WSI for sunlight, moonlight, and starlight conditions.

The Day/Night WSI is fully automated, and acquires data continuously 24-hours a day. It has been environmentally hardened, and there are versions of the D/N WSI running in the desert, Arctic, tropics, and other environments. The lens covers the full upper hemisphere, down to just below the horizon (with a field of view of 181.5 degrees typically). The system uses a Series 200 or Series 300 Photometrics 16-bit CCD camera. This camera has a three-stage Peltier cooler on the chip, and is cooled to approximately –40C. The full dynamic range of the WSI system is over 10 logs (a factor of 10^{10}) due to a combination of the dynamic range of the camera, the neutral density offset filters, changes in camera exposure time, and changes in spectral filters. With this dynamic range and low noise camera, the WSI acquires imagery under daylight, moonlight, and starlight; under starlight, even the darkest part of the sky between stars has a signal to noise ratio of 50 or more under most conditions.

A dual-wheel filter changer enables adjusting flux levels with neutral density filters, and changing spectral filters. The spectral filter options are blue (450 nm), red (650 nm), NIR (800 nm) and open hole for use at night. The solar/lunar occultor provides full shading of the front optics, in order to minimize stray light. (A much smaller shade could provide shading such that the sun does not directly illuminate the CCD, however we feel that it is vital, in order to acquire high quality data, to shade the full extent of the front optics.) This of course means that the solar/lunar occultor must be held at a reasonably large distance from the lens so that it does not obscure excessive fractions of the sky dome. A new occultor has recently been designed, which should shade only 2-3% of the upper hemisphere while still shading the full optics.

3. WSI DATA PRODUCTS

The primary WSI data products are the displayed images such as shown in Fig. 3a, the cloud fraction images shown in Fig. 3b, the total cloud fraction and cloud fraction in selected regions of interest, and absolute radiance distribution. The ability to extract earth-to-space beam transmittance at night is also working in its preliminary version. The raw data are automatically converted to an 8-bit display on the computer monitor. This displayed imagery is useful for a number of applications even without further processing. For example, some of our sponsors have used this data to evaluate the sky condition visually during tests, for determining an appropriate window of opportunity for specific tests, and for evaluating conditions along satellite tracks during tests.

A number of current and potential applications require an automated cloud algorithm. These applications include automated analysis of cloud fraction for modeling, automated assessment of cloud conditions in specific regions of the image, and potentially automated alarms. During the daytime, the cloud decision algorithm identifies each pixel as opaque cloud, thin cloud, no cloud, or no data. Results of the daytime cloud algorithm are shown in Figure 3.

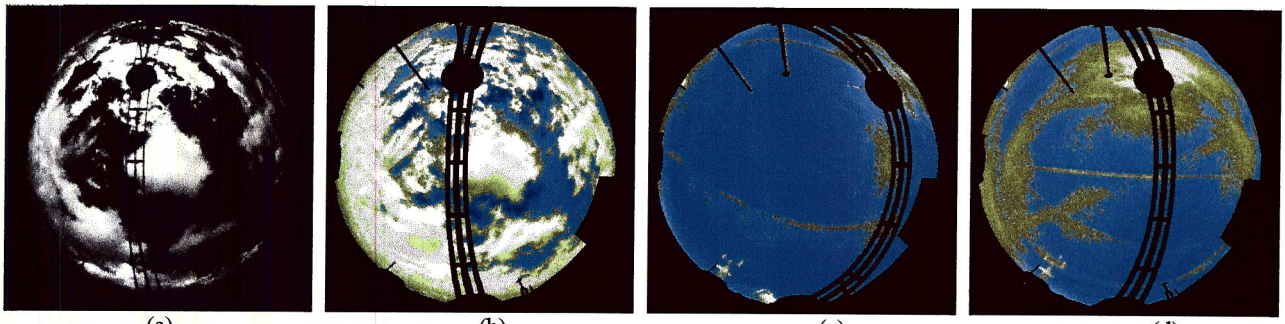

Figure 3: Day Cloud Algorithm Result: a) Raw data with cumulus or alto-cumulus clouds; b) Cloud decision result for image a, where white is optically opaque, yellow is optically thin, blue is no cloud, and black is no data; c) Cloud decision result for thin clouds associated with contrails; d) Cloud decision result 2 hours after image c.

For opaque clouds, the daytime cloud algorithm is based on the red/blue ratio at each pixel. For thin clouds, it is based on a ratio between the measured red/blue ratio and the pre-determined red/blue ratio for a clear sky for the same solar zenith angle. That is, the thin cloud algorithm takes into account the variation in spectral signature of the sky as a function of look angle and solar zenith angle. The algorithm generally works well for opaque clouds and moderately thin clouds. Under hazy conditions, however, it has difficulty distinguishing very thin clouds from the haze or aerosols. An

upgrade to use the NIR filter data is in development with the Day WSI, and we hope to apply the new work to the Day/Night WSI in the future. It should also be mentioned that DOE's Atmospheric Radiation Measurement (ARM) Program uses an alternative algorithm, which is beyond the scope of this article.

Most of the military D/N WSI systems developed for Starfire Optical Range and other sponsors have the cloud algorithm running in near-real time. These systems also use a first-version night algorithm. A typical night algorithm result is shown in Figure 4. The night algorithm currently uses 357 cells in the sky, and makes an assessment within each cell of the cloud condition. We consider the algorithm result shown in Figure 4 to be somewhat preliminary. It was based on detection of stars from a star library, in conjunction with an angular calibration of the image. The angular calibration is accurate to within approximately half a pixel. For each star, the image is inspected to determine if the star can be detected. If it is detected, the area under the point spread function for the star is evaluated, and a contrast between this integrated signal and the background is determined. The clouds are identified using contrast thresholds that depend on star magnitude, moon phase, and look angle. We would like to update this algorithm using the transmittance work described below. We also feel that in the future it should be possible to develop a higher spatial resolution night algorithm based on the absolute radiance.

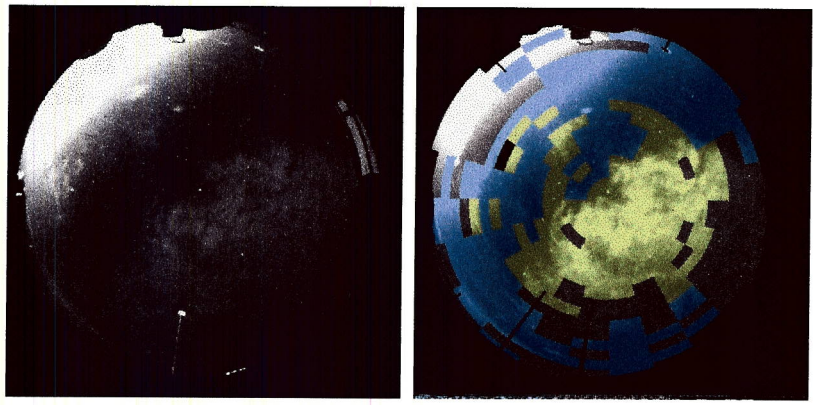

(a) (b)

Figure 4: Night algorithm results: a) Raw image; b) Cloud decision image.

Using these automated algorithms, it is possible to design systems that provide automatic alarms for unacceptable test conditions, and assess a variety of satellite tracks or other regions of the sky to make optimized test decisions. The data can also be used for studying CFLOS statistics and for other modeling efforts.

Another standard data product of the WSI is the absolute radiance distribution. Each pixel in the camera is calibrated, so the instrument provides approximately 180,000 measurements of radiance simultaneously. The systems are calibrated in each wave band. We are quite careful with the calibrations, measuring the impact of non-linearity, shutter opening time, non-uniformity, lens roll-off, pixel cross-talk, and so on. Absolute calibrations are traceable to NIST. A discussion of the calibration is beyond the scope of this paper, however the calibrations are generally self-consistent to within fractions of a percent. The lamps are accurate to 2-3%, depending on age, so we believe that the overall calibration is generally accurate to within 3 – 5%. At the present time, the sky radiance distributions are processed in archival mode, and are not an automated real-time product. Conversion to a real-time product, if an application required it, is straight forward.

The most recent data product is the distribution of earth-to-space beam transmittance over the night sky. Although a detailed development of the theory is beyond the scope of this paper, we can present an overview of the technique and the results. The 5th edition NSSDC Bright Star Catalog (Hoffleit, 1991) is used to determine the magnitude and color temperature of stars down to visual magnitude 7.96. From these values, the expected inherent irradiances of the stars in the WSI open hole passband are determined. By "inherent", we mean the effective irradiance of the stars above the atmosphere. A very accurate angular calibration of angle in object space vs. pixel position in image space enables a reasonably accurate determination of the association between the stars in the image, and the stars in the library. The images are calibrated for absolute radiance. We have found that the Point Spread Function of the atmosphere and the optics can be reasonably well described by a Gaussian with a width of 0.45 pixels over the full image. By integrating over this PSF and subtracting the background, we can make reasonably good determinations of the apparent irradiance of the stars in the image. By "apparent', we mean the irradiance as seen from the observer or WSI position. The ratio of apparent to inherent irradiance should yield the total earth-to-space beam transmittance.

Figure 5 shows the resulting relationship when the inherent and apparent star irradiances are compared. In this data set of 1555 stars of magnitude down to approximately 3.9, the correlation is very good, with a correlation constant of .968.

If stars down to a magnitude of approximately 7.0 are used, yielding a data set of nearly 33,000 stars for this night, the correlation is .847. We believe that this may be due to uncertainties in the star magnitude values. The ability of the WSI to observe the full upper hemisphere with a calibrated sensor simultaneously is a very strong capability, and should enable us to further improve the inherent star irradiance values.

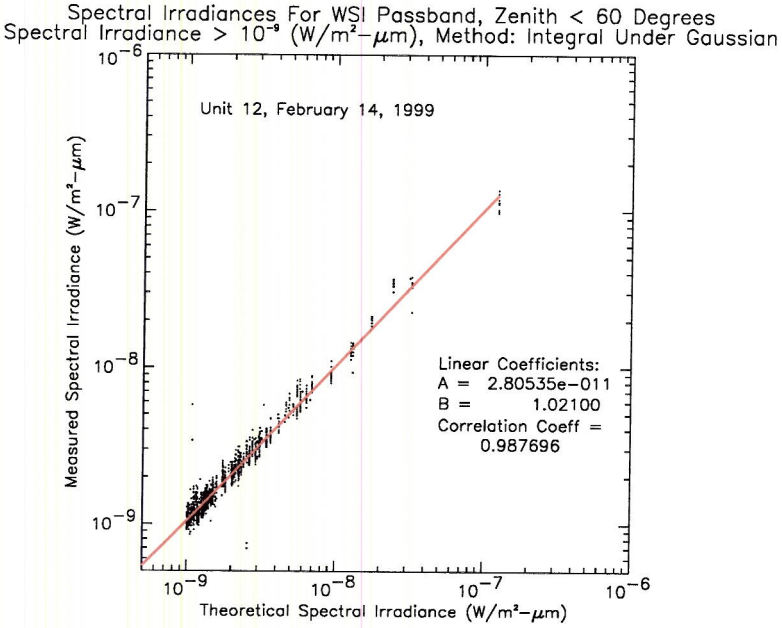

Figure 5: Observed relationship between the measured, or apparent star irradiance, and the computed, or inherent star irradiance on a clear night.

The resulting transmittance map is shown for a sample case in Figure 6. The raw data are shown in image a, and the total earth-to-space beam transmittance is shown in image b. For this plot, we used stars to magnitude 6.0 that were not too close to other stars. We determined from a series of clear nights that an earth-to-space beam transmittance of approximately 0.8 is typical for this filter; the residual transmittance corrected for the clear night transmittance is shown in image c. Although it is not obvious in this display of the raw data, there were clouds present in the bright band near the horizon. Although the variance in these results is somewhat higher than we would like, we are very pleased with this as a first result, and feel that it can be improved by modifying the inherent star values based on measurements on clear nights. Similar simultaneous measurements of the full star field in a variety of wavelengths from high altitude could be quite useful.

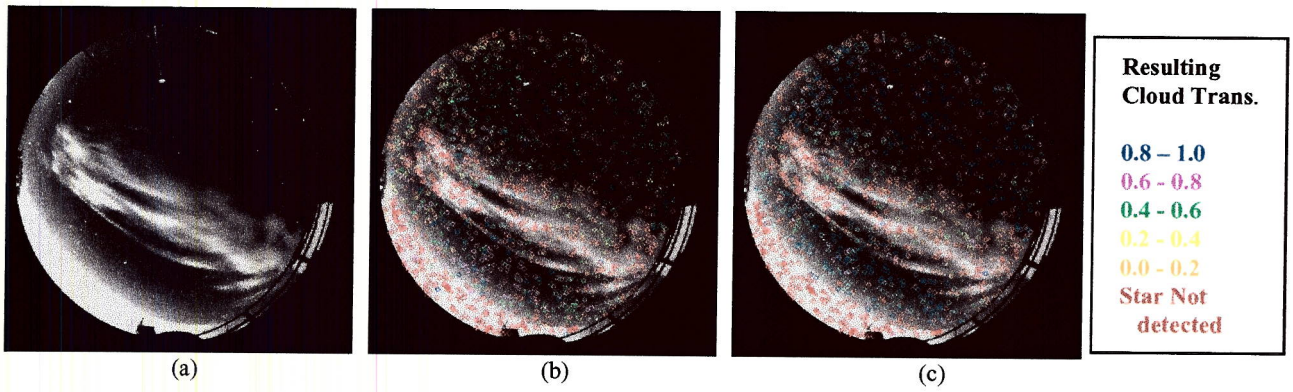

Figure 6: Transmittance Map Results: a) Raw data, b) the total earth-to-space beam transmittance result, c) the residual transmittance corrected for a clear-night vertical earth-to-space transmittance of 0.8.

4. CUSTOMIZED WSI'S FOR SPECIALIZED APPLICATIONS

Over the years, several versions of the WSI have been designed and deployed. This section will provide a very brief overview of these systems. Most of the WSI systems utilize cable bundles communicating between the controller and the sensor, and require that the sensor be within 230' of the controller. For the Day/Night WSI shown in Figure 7, the controller package was integrated into the sensor environmental housing. As a result, it can be sited remotely from the user. The WSI sends data via Ethernet link to a second computer, where data are processed in near-real time. The

computer can also accept instructions from another computer controlling another application or model. This computer can request moving regions of interest (ROI), and the WSI returns the information on cloud cover within this ROI to the user or model.

The original Day WSI developed in the 80's is obsolete, and a new version of the Day WSI has been developed based in part on the upgrades used in the Day/Night WSI systems. The Day WSI is shown in Figure 8, and an image near sunset (with the occultor nearly below the horizon) is shown in Figure 9. This system acquires imagery in seven user-selected passbands in the visible and NIR at approximately 1024 x 1024 resolution. It provides calibrated radiance distributions in all wavebands, as well as cloud fraction. This is the system for which a new daylight cloud algorithm is in development. It is further documented in Shields et al (2003 a). Like the Day/Night WSI, it provides high quality, fully shaded imagery appropriate for a variety of applications.

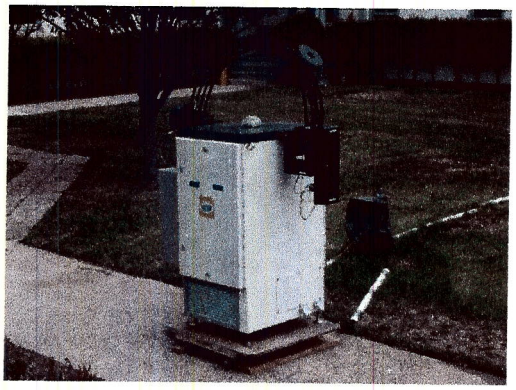

Figure 7: Day/Night WSI for Remote Sites

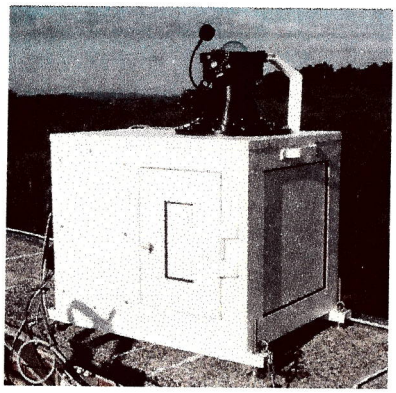

Figure 8: Day Visible/NIR WSI

Figure 9: Raw image from Day WSI

A small calibrated fisheye imaging system has recently been developed for airborne use on a UAV. It consists of two camera packages, a visible system near 645 nm using Silicon CCD technology, and a NIR system near 1610 nm using InGaAs CMOS technology. The NIR camera and a visible image are shown in Figure 10. Both of the systems are fully calibrated, to provide the radiance distribution of the lower hemisphere, and the cloud top radiances in particular. Although this was designed for use with the ARM program, we feel that it has great potential for tactical and other military applications. This system is documented in Feister et al (2000) and Shields et al (2003b). We have also determined how we could develop similar systems at 3 –5 μm and 8 – 12 μm.

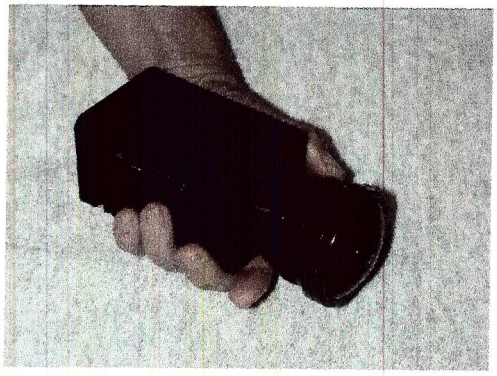

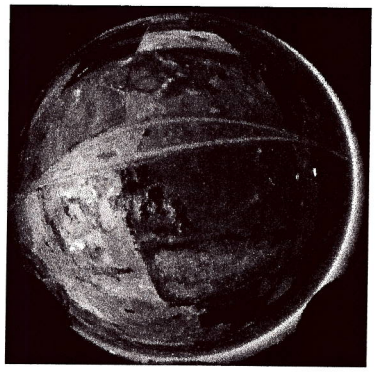

Figure 10: One of two airborne fisheye systems designed for use with a UAV. The first figure illustrates the camera that acquires images near 1.6 μm in the NIR, and the second image illustrates data from the visible system near 650 nm.

5. CLOUD FREE LINE OF SIGHT STATISTICAL STUDY

An early version of the Day WSI developed by MPL was fielded in the mid-to-late 1980's at several sites throughout the U.S., acquiring data once a minute for over two years. The data were originally acquired for support of ground-based high-energy laser applications, and approximately one year of data from each of several of the sites were processed through the cloud algorithm in those years. These processed data were recently further processed to extract statistics on Cloud Free Line of Sight (CFLOS) with funding from the Air Force's Starfire Optical Range. This section presents a sampling of the results extracted from this data set.

The processed data consisted of cloud algorithm results such as those shown in Figure 11. This was a fairly early version of the algorithm, but comparisons with observers over a limited test case showed very good agreement with the observer. Approximately 82,000 images such as given in Figure 11 were available at 10-minute intervals, and used for the CFLOS determinations. Approximately 820,000 images at 1-minute intervals were used for the Persistence studies.

Figure 11: Sample Day WSI Cloud Algorithm Data Product for CFLOS Study

The PCFLOS data were extracted as a function of cloud fraction, zenith angle, station location, and season. Figure 12 shows some very preliminary data extracted from a limited sample of WSI data, in comparison with two models. The straight line "model", one minus cloud fraction, represents the relationship that might be expected if clouds were uniformly small, evenly distributed, and essentially had no physical thickness. If one takes into account the thickness of clouds, the result is similar to that shown by the curve labeled SRI model. These results were provided to us courtesy of TASC, Inc. The WSI data showed an interesting drop near 80% cloud cover. A more detailed study of the WSI, based on 24,000 cases near White Sands Missile Range (WSMR) shows the same behavior in Figure 13. We believe this behavior is real, and reflects the fact that clouds often are not evenly distributed small clumps. If the 80% cloud cover is associated with a front, and 80% of the sky is covered, then the zenith will also not be cloud free. This behavior is of course inverted near the horizon, as shown in the 75 degree zenith angle curve in Figure 13.

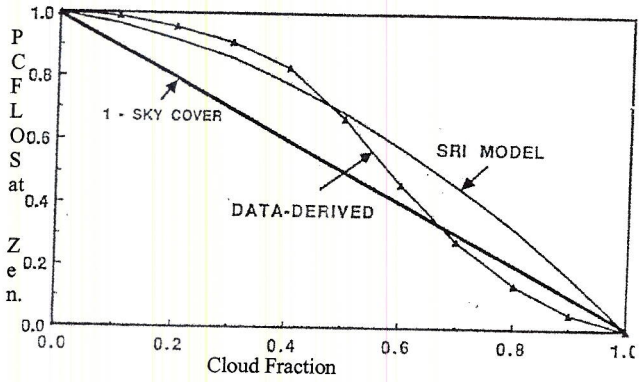

Figure 12: Model and Sample WSI Data for PCFLOS At the zenith as a function of Cloud Fraction.

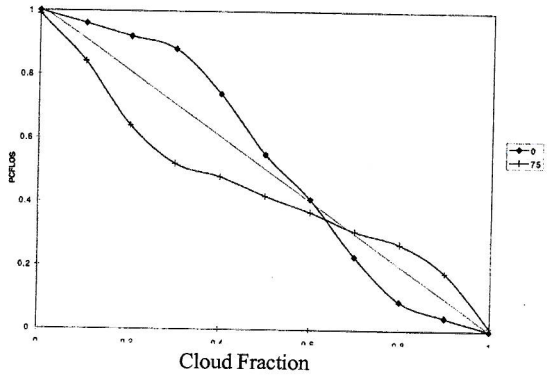

Figure 13: PCFLOS at Zenith and at 75 degrees zenith angle as a function of Cloud Fraction; data from WSMR, 24,000 cases.

Another type of data product extracted from the CFLOS data is the conditional probability. As an example, in Table 1 column 2, we show the probability that the sky is clear in the direction toward GOES-8, for each of 5 sites. These probabilities range from around 66% for the desert sites, to 35% for the coast of Florida. However, if we look at the conditional probility that the line of sight towards GOES-8 is clear given that the line of sight toward Polaris is clear, now the probabilities increase to 92% to 84%.

Table 1
Conditional Probability for a
Cloud Free Line of Sight to GOES-8

Location	PCFLOS in GOES-8 Direction	PCFLOS for GOES-8 if Polaris is clear
Albuquerque, NM	0.66	0.92
White Sands, NM	0.63	0.90
Columbia, MO	0.46	0.86
Malmstrom AFB, MT	0.38	0.72
Malabar Tracking Station, FL	0.35	0.84

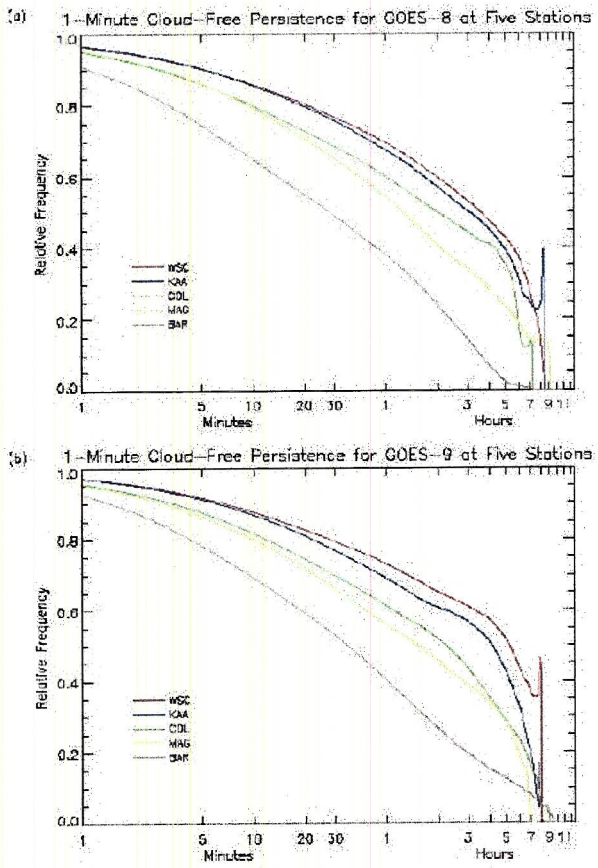

Figure 14: Cloud-free Persistence results for yearly Averages at five stations and in two directions.

It is also interesting to evaluate the persistence. Figure 14 shows a sample persistence result. For those cases which had a clear line of sight in a given direction at Time T_0, we determined what fraction of these cases remained clear throughout the interval from time T_0 to time T. The upper plot shows five stations for the GOES-8 direction, and the lower plot shows the GOES-9 direction. At some of the stations, such as those in the desert, the probability of persistence was quite high. For example, at WSMR, the probability fell to 50% only after over 5 hours. At the Florida site, the probability fell to 50% after less than an hour. Similar studies were made as a function of season, and also studies of the persistence of cloudy conditions were made. These results are shown in Table 2.

Table 2
Persistence Results:
Time (hr) Required for Yearly Persistence
Probabilities for Polaris to drop below 0.5

Location	Cloud-free	Cloudy
Albuquerque, NM	4.1	1.1
White Sands, NM	5.1	0.7
Columbia, MO	3.1	2.6
Malmstrom AFB, MT	1.5	2.9
Malabar Tracking Station, FL	0.8	0.4

In Table 2, the persistence of cloud-free conditions is quite long for the desert sites, and shorter for the other sites, as expected. The persistence of cloudy conditions is short for the desert sites. For the first four sites in the table, the cloudy persistence increases, as the cloud-free persistence decreases. However, for the coastal Florida site, where we often seemed to observe small fast-moving clouds, both the cloud-free and cloudy persistences were short.

While the above CFLOS and Persistence data give a small sampling of the type of statistics that were extracted from the WSI data-base, there are many statistics that can be extracted. For example, we evaluated multi-station behavior, in terms of both CFLOS and Persistence, and conditional probabilities such as the time persistence for having N stations with a clear line of sight, if M stations were available.

6. A TACTICAL FULL SCENE IMAGER (PATENT PENDING)

Another development that has come out of the Whole Sky Imager family of systems is the concept for a Tactical Full Scene Imager. In its simplest concept, this system uses a single fisheye lens with a beam splitter behind the lens to create two image planes, as shown in Figure 15. One of the image planes is used to provide an image of the full hemisphere scene, either using a tapered fiber optic bundle as shown, or using a lens, or by using imaging directly onto a chip if feasible. The second image plane is interrogated with a microscope objective, in order to provide a high-resolution view of a portion of the scene.

This concept is demonstrated in Figures 16 and 17. Figure 16 shows the full fisheye view (180 degrees in field of view) of the test room. Image (a) has been displayed to show the room, and image (b) has been displayed to show the optical target.

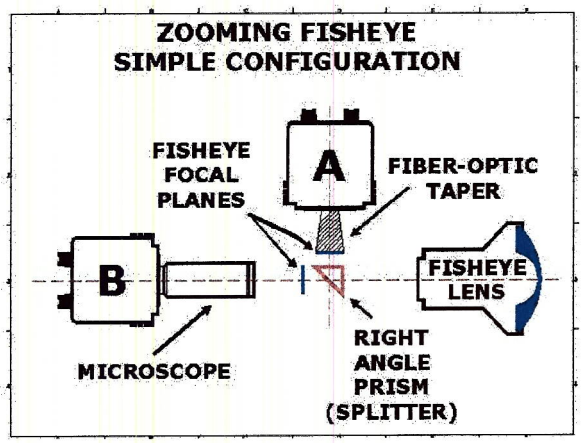

Figure 15: The simplest concept for the Tactical Full Scene Imager concept

Figure 17 shows the image through the microscope objective. The image plane has a high spatial frequency content, well beyond that which is acquired in the imagery shown in Figure 16. As a result, it is possible to extract high resolution imagery with a behind-the-lens optical zoom using a microscope objective. Image (b) of Figure 17 shows a small portion of image (a) further enhanced using electronic zoom. Image (c) of Fig. 17 shows the best we could achieve with electronic zoom alone.

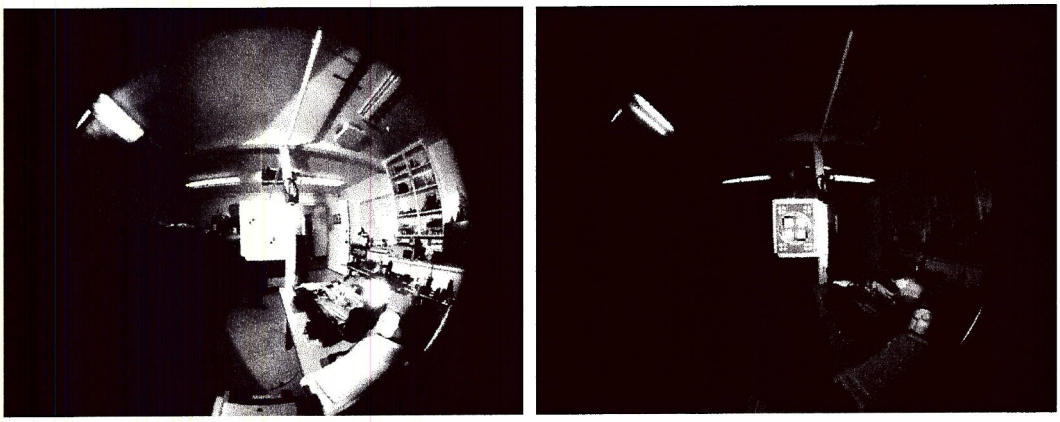

(a) (b)

Figure 16: Image of the full scene in a test room: a) displayed to show the room, b) displayed to show the target

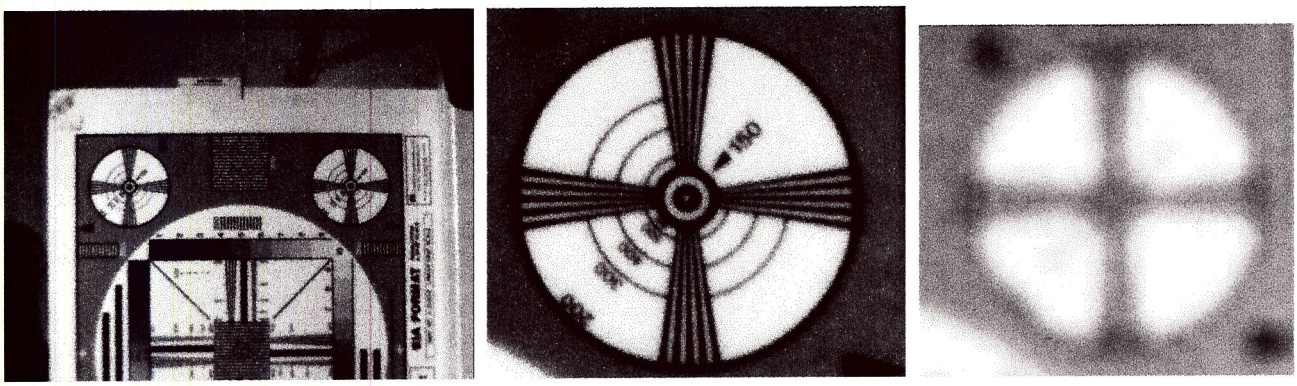

(a) (b) (c)

Figure 17: Images using Zooming: a) Image of the image plane through a microscope, b) Image of the target using both optical and Electronic zoom, c) Image of the target using electronic zoom alone.

This concept could be used with human interaction, or could be fully automated. For example, a human in a tank could view an image such as in Figure 16, chose an area of interest using a touch-screen monitor, and the system could display the high resolution view of the selected area of interest. Similarly, a motion detection algorithm could be used to automatically select the area of interest. A number of different lens and camera configurations is possible. For example, use of three fisheye lenses would enable the full spherical surround to be viewed continuously with a completely staring system. The system should be far more robust, dust-resistant, and covert in comparison with external optical zoom, and we have developed methods for doing very fast changes to the region of interest. The system currently has a patent pending, and is in mock-up stage. We feel that it has many applications both for tactical applications in unattended ground sensors, tanks, and ships, as well as for now-casting in the battlefield environment.

7. SUMMARY

The Whole Sky Imagers have been developed for a number of applications, including military and general research applications. The data products can include the raw images, cloud decision images, and absolute radiance distributions. More recently the ability to determine the distribution of beam transmittance over the full sky at night has been developed but not yet integrated into the real-time processing software. Several versions of the instrument have been developed, including a Day/Night WSI, Day/Night WSI with automated real-time processing, Day WSI, and an airborne fisheye system. Cloud Free Line of Sight statistics have been extracted from part of the WSI data base. Concepts for tactical systems and now-casting are in development.

8. ACKNOWLEDGEMENTS

We would like to express our appreciation to the Starfire Optical Range, for their support of much of this work, as well as for providing partial support to enable the presentation of these results. We would especially like to thank Ann Slavin for her advice and technical support in this work. In addition, we would like to thank Dr. Tim Tooman at Sandia National Laboratories, and the DOE's Atmospheric Radiation Measurements Program administered by Battelle's Pacific Northwest National Laboratories, for their support of much of the D/N WSI development. Thanks also to the Air Force Research Labs, and to Deutsche Wetterdienst, the German Weather Service which supported some aspects of the research. We would like to recognize Roper Scientific, for their assistance with the Photometrics camera products.

9. REFERENCES

1. R. W. Johnson, W. S. Hering, and J. E. Shields, *Automated Visibility and Cloud Cover Measurements with a Solid State Imaging System*, University of California, San Diego, Scripps Institution of Oceanography, Marine Physical Laboratory, SIO 89-7, GL-TR-89-0061, NTIS No. ADA216906, 1989.

2. J. E. Shields, R. W. Johnson, and T. L. Koehler, *Automated Whole Sky Imaging Systems for Cloud Field Assessment*, Fourth Symposium on Global Change Studies, American Meteorological Society, 1993.

3. J. E. Shields, R. W. Johnson, M. E. Karr, and J. L. Wertz, *Automated Day/Night Whole Sky Imagers for Field Assessment of Cloud Cover Distributions and Radiance Distributions*, Tenth Symposium on Meteorological Observations and Instrumentation, American Meteorological Society, 1998.

4. R. W. Johnson, W. S. Hering, J. I. Gordon, B. W. Fitch, and J. E. Shields, *Preliminary Analysis and Modeling Based Upon Project OPAQUE Profile and Surface Data*, University of California, San Diego, Scripps Institution of Oceanography, Visibility Laboratory, SIO Ref. 80-5, AFGL- TR-0285, NTIS No. ADB-052-1721, 1980.

5. Hoffleit, E.D., and W.H. Warren Jr., *The Bright Star Catalogue.* 5th ed. New Haven,Conn.: Astronomical Data Center and Yale University Observatory, 1991.

6. Feister, U., Shields, J., Karr, M., Johnson, R., Dehne, K. and Woldt, M, *Ground-Based Cloud Images and Sky Radiances in the Visible and Near Infrared Region from Whole Sky Imager Measurements*, Proceedings of Climate Monitoring – Satellite Application Facility Training Workshop sponsored by DWD, EUMETSAT and WMO, Dresden 2000.

7. J. E. Shields, R. W. Johnson, M. E. Karr, A. R. Burden, and J. G. Baker, *Daylight Visible/NIR Whole Sky Imagers for Cloud and Radiance Monitoring in Support of UV Research Programs*, International Symposium on Optical Science and Technology, SPIE the International Society for Optical Engineering, 2003a.

8. J. E. Shields, R. W. Johnson, M. E. Karr, A. R. Burden, and J. G. Baker, *Calibrated Fisheye Imaging Systems for Determination of Cloud Top Radiances from a UAV*, International Symposium on Optical Science and Technology, SPIE the International Society for Optical Engineering, 2003b.

MARINE PHYSICAL LABORATORY, 0701
of the Scripps Institution of Oceanography
San Diego, California 92152-6400

Technical Memorandum **AV03-030t**
To: Atmospheric Optics Group 19 May 2003
From: A.R. Burden
Subject: Improvements Made to Starlight-Based WSI Cloud Algorithm

This memo describes the continued development of a nighttime, starlight-based cloud algorithm included in the day-night WSI system. Related information regarding automatic detection of stars in nighttime imagery can be found in Tech. Memos AV98-040t, AV98-042t, AV99-043t, and AV99-044t. Memo AV99-044t describes the original version of the starlight-based cloud algorithm. The improvements discussed here represent the initial attempt at a working star-based nighttime algorithm that can be used under all moonlight conditions. We feel that further upgrades are possible, and we have not had extensive time to test the current algorithm. However, this version of the algorithm was integrated into the real time cloud processing code and was included in the version of the algorithm that was delivered to Air Force in March 2001. The software has been in use since that time. Although we do not normally see the data or processed results, reports from the field indicate that the algorithm is working to their satisfaction.

The primary modifications to the algorithm described here include the addition of an occultor mask to allow use of the software during moonlit nights, and magnitude and zenith angle dependent thresholds that allow for distinguishing cloud-free, opaque cloud-covered, and thin cloud-covered regions. Additionally, the new version dark-corrects raw imagery prior to analysis. The number of cloud identification cells was increased from 257 to 357, as each scene is analyzed to a zenith angle of 90°, rather then the previous 70°. Other modifications will be discussed in the text below. The new nighttime cloud detection software is named StarCloudAlg.

Occultor and Horizon Masks

It is important to know what areas of a WSI image are part of the instrument or horizon features in order to accurately determine whether regions in a WSI image are cloud-free or overcast. This is especially true for WSI images collected under moonlight, where the WSI occultor and ladder covers a significant percentage of the image. An occultor masking method based on one written by Tim Tooman from ARM was added to StarCloudAlg. Constant parameters, such as the occultor rail and rung widths, as well as arc and trolley positions given in the WSI image header, are used to mask the expected locations of the occultor and ladder. Since the horizon features are relatively constant, it was relatively simple to create a horizon mask. An IDL routine was written to interactively select regions of the image to incorporate into the mask. The software, called HorizonMaskEditor.pro, may be used to create and save a horizon mask for any site. Figure 1 shows an example of an SOR image with the horizon and occultor masks applied.

Occultor and Horizon Mask for SOR Night Image
Image Collected February 27, 1999, 0400 UT

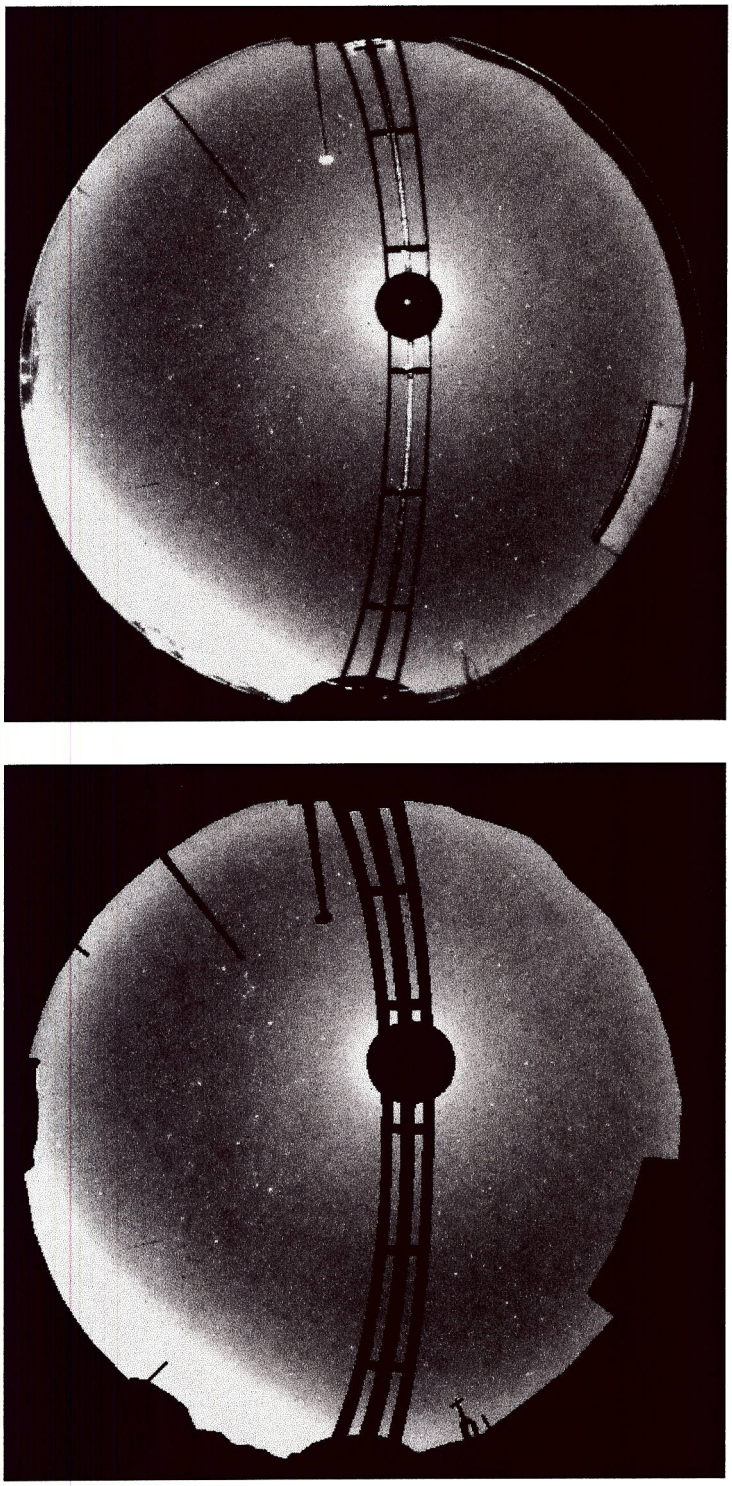

Figure 1. Top: Sample SOR image with moon and occultor in field of view. Bottom: Same image with horizon and occultor masks overlayed.

Night Algorithm Background

As discussed in Memo AV99-044t, the previous version of the night algorithm, called GetStarData, used a threshold scheme to distinguish clear regions from overcast regions. The algorithm used a high precision geometric calibration to determine the relationship between angle in object space, and pixel location in object space. It used a NASA star library, and predicted the approximate position of stars in the imagery (as a function of instrument location and image time). The imagery was then evaluated near the expected position, to locate the presence of a star. We had found that the star signature in the image could be adequately represented by a Gaussian function of width .45 pixels. Thus the search for the star in the image was based on a search for this Gaussian point spread function. The signal was defined as the area under the Gaussian, minus the background determined by the Gaussian best-fit program.

Basically, any star with a signal to background contrast less than or equal to 0.18 and a point spread function (PSF) outside the range 0.3-0.8 was considered obscured by cloud. A star with a contrast greater than 0.18 and PSF in the range 0.3-0.8 was considered to be cloud-free. While this method effectively identifies opaque cloud in many images, it does not distinguish stars covered by thin cloud from those that are cloud-free. Additionally, the method does not account for differences in star magnitude and image stray light effects. Both of these factors play an important role in determining the expected contrast for a star.

We felt that in the long run, the best algorithm could be devised using data with absolute calibrations. However, we felt that this would take too long in the short run. It was very important to get an adequate night algorithm fielded quickly. We felt that our best approach would be to modify the existing algorithm to take better account of the effects discussed above.

When a star is identified in an image using the algorithm, the primary parameters that are determined are the star peak and background values, and consequently, the peak to background contrast. As mentioned in the previous paragraph, the many different factors contributing to star signals reaching the instrument make using a constant contrast threshold ineffective for classifying stars. One way to use contrast to distinguish cloud was to develop a threshold method specific to the characteristics of the SOR site where the algorithm would be applied. For this case, star contrast results for cloud-free and cloud-covered images, as well as sky background data, were used to determine threshold models that are a function of star magnitude, moon phase, and zenith angle (and in some cases, azimuth angle).

Figures 2 and 3 illustrate how the contrast for a particular star can vary with zenith angle and moonlight. Each line represents data for a single star collected over one cloud-free night. When contrast for a given star is plotted against zenith angle, the pattern is consistently one of contrast decreasing with zenith angle up to a point near 80°, followed by increasing contrast. As shown in a later section, the sky background signal increases with zenith angle, and that plays a part in the decrease in the contrast closer to the horizon. The left half of each figure includes a sample of stars with visual magnitudes < 3, while the right half includes a sample of stars with visual magnitudes between 3 and 4. Figure 2 includes data collected on a night with no moon, while Figure 3 includes data collected on a night with a full moon within the field of view. As expected, contrast is lower for higher magnitude stars, as evidenced by comparing the left hand

plot with the corresponding right hand plot. Because of the enhanced sky radiance due to scattering of the moonlight, contrasts on the moonlit night are considerably lower then those from the moonless night. One other important thing to note is in the top part of Figure 2. At a zenith angle of about 55° is a cluster of points with contrast varying between 3.5-5. These points represent Polaris, which, of course, acts like an axis point that the sky 'revolves' around. Clearly, some variability in contrast can occur even for stars that stay essentially in the same sky location under consistent cloud free conditions.

Cloud-Free Contrast Thresholds

Considering the observations noted above, developing a reasonably accurate threshold technique for distinguishing cloud-free and cloudy regions must incorporate the visual magnitude and zenith angle of the star in question, as well as the presence or lack of moonlight. To further complicate things, part of every image from the SOR site is significantly affected by stray city lights. The impact of this is discussed below, but unless otherwise noted, data presented here include only those stars found in the azimuth angle range 0-270°. Stray light affects are worse for azimuth angles in the range 270-360°, and these data were often handled separately, requiring separate contrast thresholds specific to that part of the image.

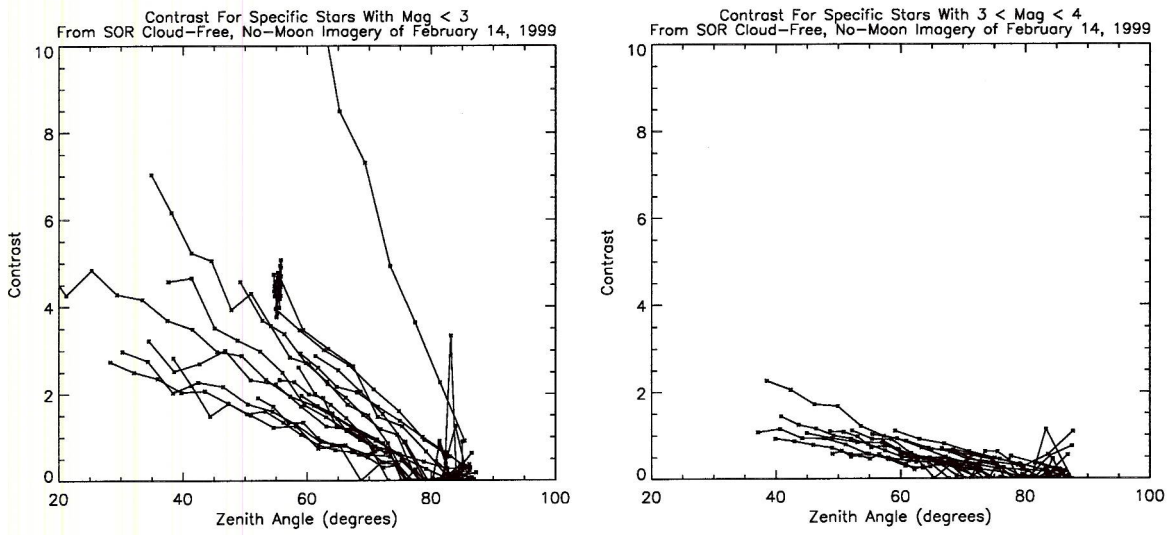

Figure 2. Contrast as a function of zenith angle for specific stars from composite of cloud-free, no-moon images. Left half includes sample stars with magnitude < 3. Right half includes sample stars with 3 < magnitude < 4.

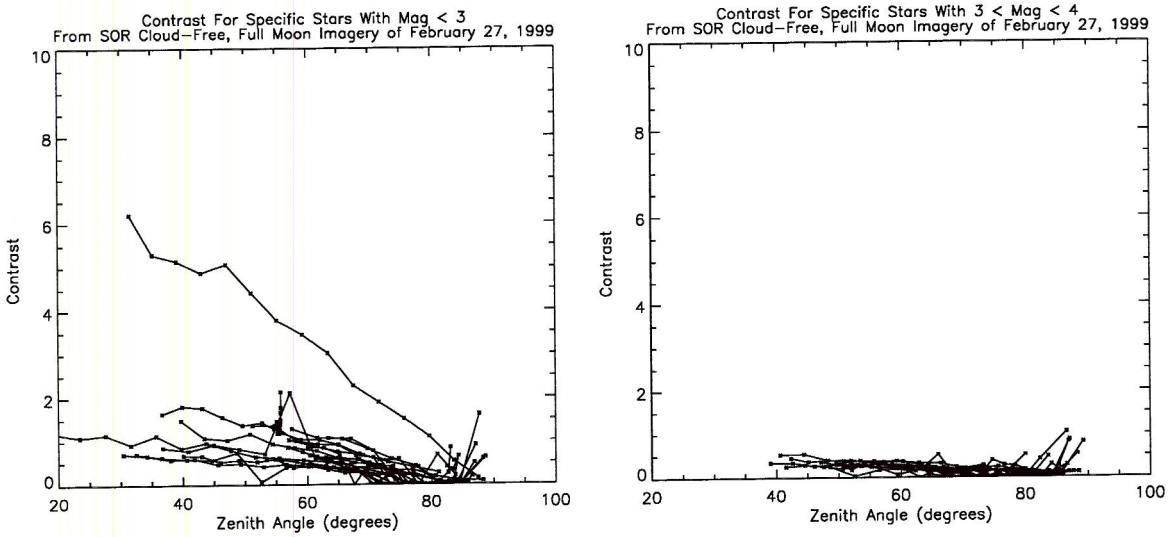

Figure 3. Same as Figure 2, except that data are from cloud-free, full moon imagery.

Examining composited data from both images with cloud-free sky and images with opaque cloud, it was determined that for lower magnitudes and lower zenith angles, at least, enough separation in contrast exists between cloud-free and opaque cloud cases that using thresholds is a reasonable approach. It was found that the behavior of cloud-free contrast as a function of zenith angle for stars within a small range of visual magnitudes could be modeled using a function similar to that used to model atmospheric transmittance as a function of zenith angle, given in Equation 1:

$$T = T_0 \tau^{\sec\theta} \qquad \text{Eq. (1)}$$

where, T is cloud-free contrast, T_0 is cloud-free contrast at the zenith point, τ is transmittance, and θ is zenith angle. τ is typically in the range 0.4-0.8. The curve is characterized by a shallow drop off at low zenith angles that becomes more pronounced at larger zenith angles. To determine T_0 and τ, the composited contrast data from cloud-free images were plotted within small magnitude ranges that represented enough data to be useful, yet not too wide that the range of contrast was too large. Examining these data showed that the modeled contrast threshold curve most closely followed the trend of the measured star contrasts when $\tau = 0.6$. Modifying T_0 changes the y-intercept for the modeled contrast threshold curve.

Figure 4 shows some example cases using cloud-free no-moon data from February 14, 1999. Each plot in the figure consists of star data within a specific magnitude range. For example, the first plot contains data for magnitudes –1.5 to 0.5, since there are so few stars to plot at such low magnitudes. For higher magnitudes, the magnitude ranges are much smaller, typically 0.1. Blue points represent those stars in the given magnitude range identified as having characteristics consistent with a cloud-free sky (Code 0). Red points represent data from images with opaque cloud, and are discussed below. The solid line in each plot is the cloud-free contrast threshold model based on Equation 1, where T has been selected so the curve closely follows the bottom of the cluster of data points. Contrast thresholds were interactively determined in this manner for star magnitudes up to 6.0. Using this criterion, stars within the given magnitude

range with a contrast greater than the threshold for the appropriate zenith angle will be identified as being cloud-free. If the contrast is less than the threshold, the star will be identified as either thin cloud or opaque cloud, depending on how low the measured contrast is. Obviously, this method will identify some thin cloud as cloud-free, since the threshold lines were chosen to be below the majority of the points. Some points appear just above the line, while others are significantly higher. This is partly due to observed variability for stars (e.g., Polaris case described above) and the finite range of magnitudes used to bin the data, and partly due to other causes not yet identified at the current stage of analysis. Attempts at determining star-specific thresholds for a small number of stars showed that the results did not change significantly from using the method described here. In any case, star-specific thresholds, smaller magnitude bin sizes, and other ways for possibly getting tighter tolerances are not really feasible due to the large time commitment in determining the thresholds. Other methods could be considered as funding allows. Figures 5 and 6 show analogous results for the half moon and full moon cases.

In each case shown in Figure 4 the threshold curve closely follows the trend of the contrasts with increasing zenith angle. Since τ is a constant, the determining factor for the threshold curve is T, the threshold contrast at zenith. For the no moon case and magnitude ranges shown here, T starts out at 45 in the first plot, drops to 22 in the second, and keeps dropping as the magnitudes increase. In order to determine the threshold to use when checking each star, we need to determine T, and then solve Equation 1 using the appropriate zenith angle. To determine T during image processing, a second model was created based on the chosen T values shown in Figure 4. The first plot in Figure 7 shows points corresponding to the selected T values and a model fit of these points, which is based on Equation 2:

$$T = e^{(a+bm+cm^2)} \qquad \text{EQ (2)}$$

where a, b, and c are model coefficients, and m is visual magnitude. Similar models are shown for data collected on nights with quarter moon, half moon, and full moon.

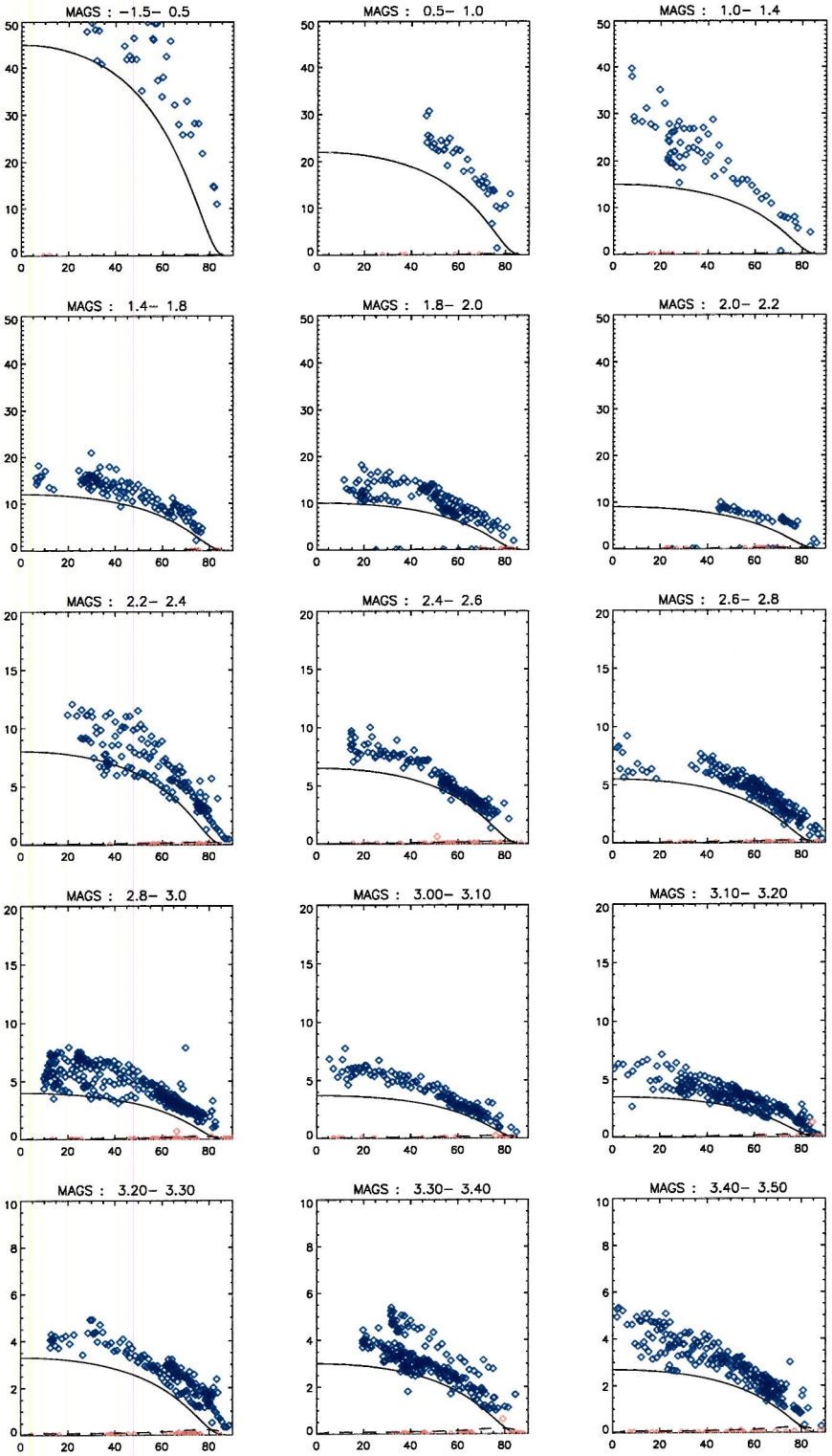

Figure 4. Contrast as a function of zenith angle for composited stars from moonless imagery. Data are separated into magnitude ranges. Blue points represent star results from cloud-free imagery. Red points represent star results from opaque cloud covered imagery. Stars above solid line are tentatively classified as cloud-free. Stars below dashed line are identified as being obscured by opaque cloud.

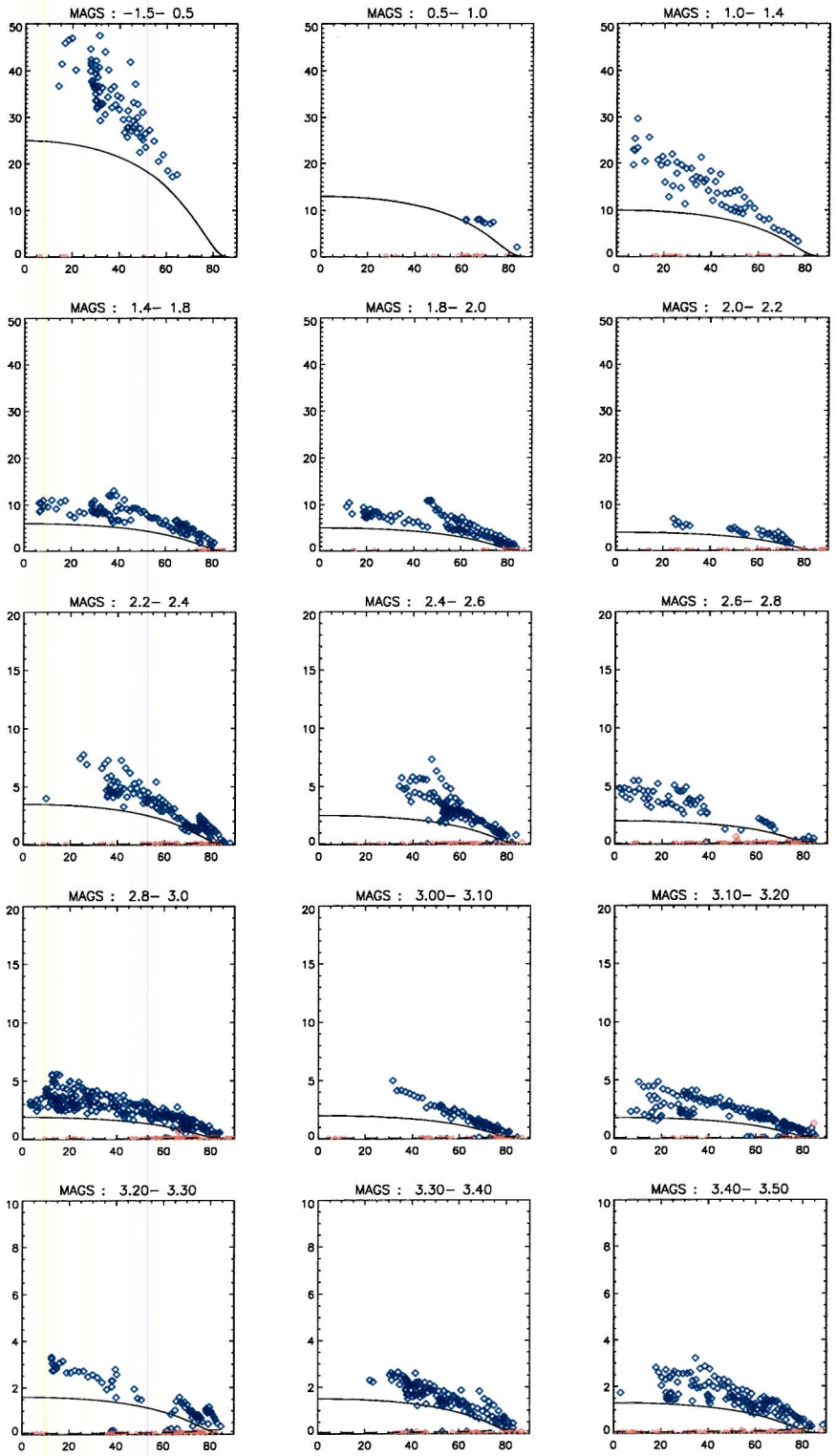

Figure 5. Same as Figure 4, except data are from images with half moon.

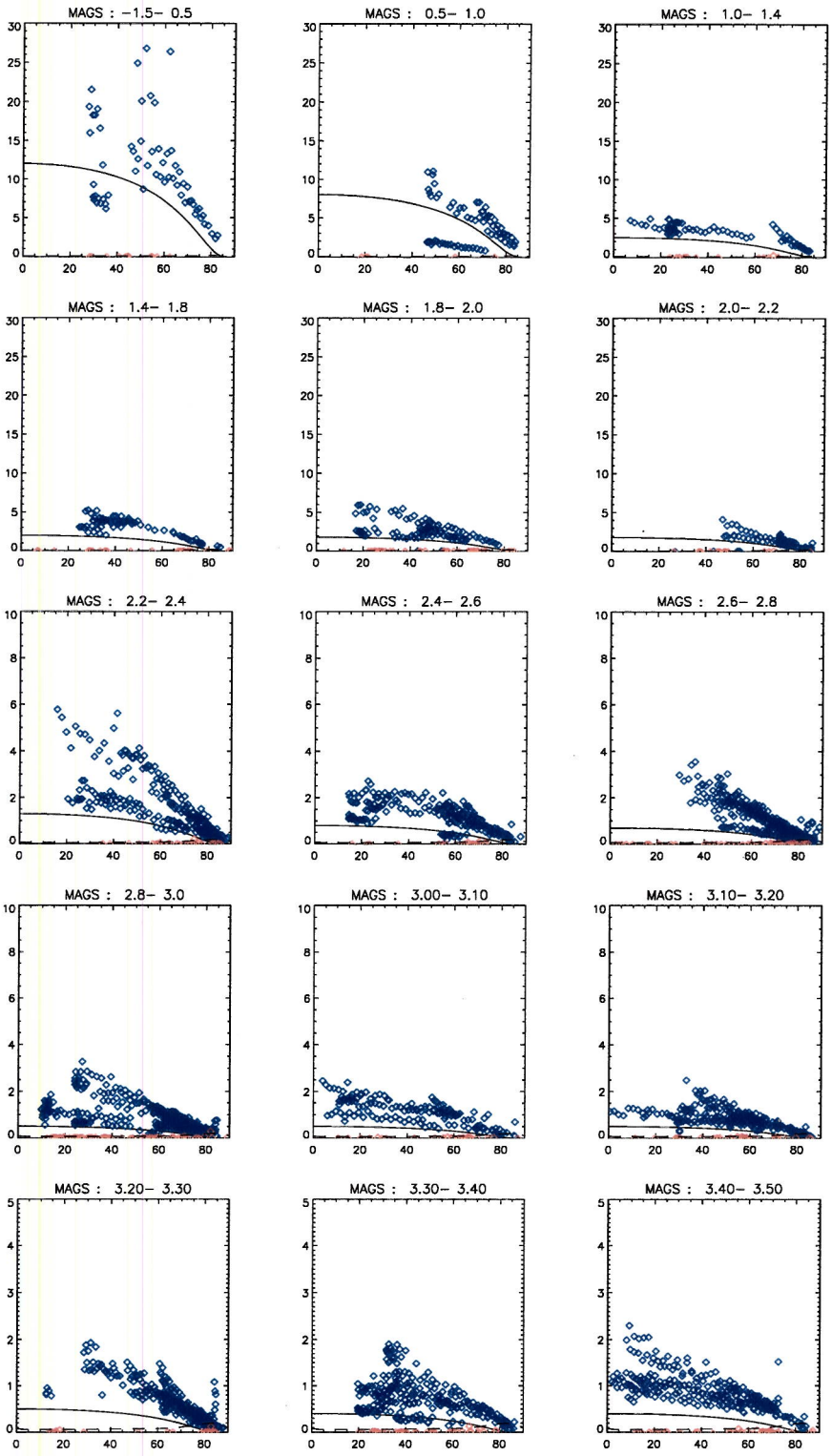

Figure 6. Same as Figure 4, except data are from images with full moon.

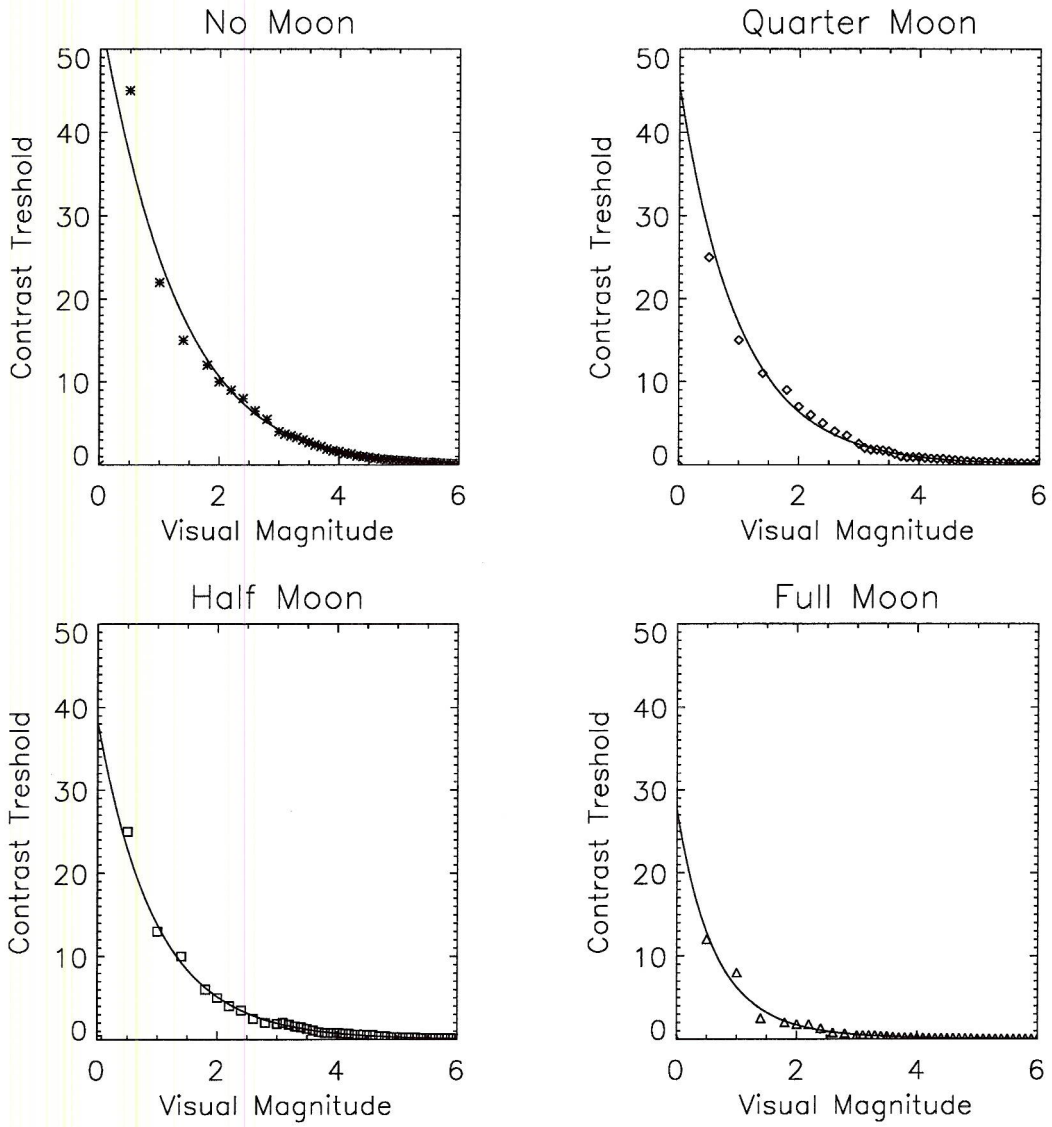

Figure 7. Star contrast at zenith point as a function of star magnitude. Solid lines represent model of data.

The task of determining T from the binned data as shown in Figures 4-6 is laborious and is not conducive to developing similar models for other sites. Assuming that the trend of contrast as function of zenith angle for other sites follows that given in Equation 1, one way to simplify the task would be to collect cloud-free contrast data from near zenith for that site and determine a model of T from those data. As an example, Figure 8 shows the model of T from Figure 7 (no-moon case), along with measured contrast results for zenith angles < 10°.

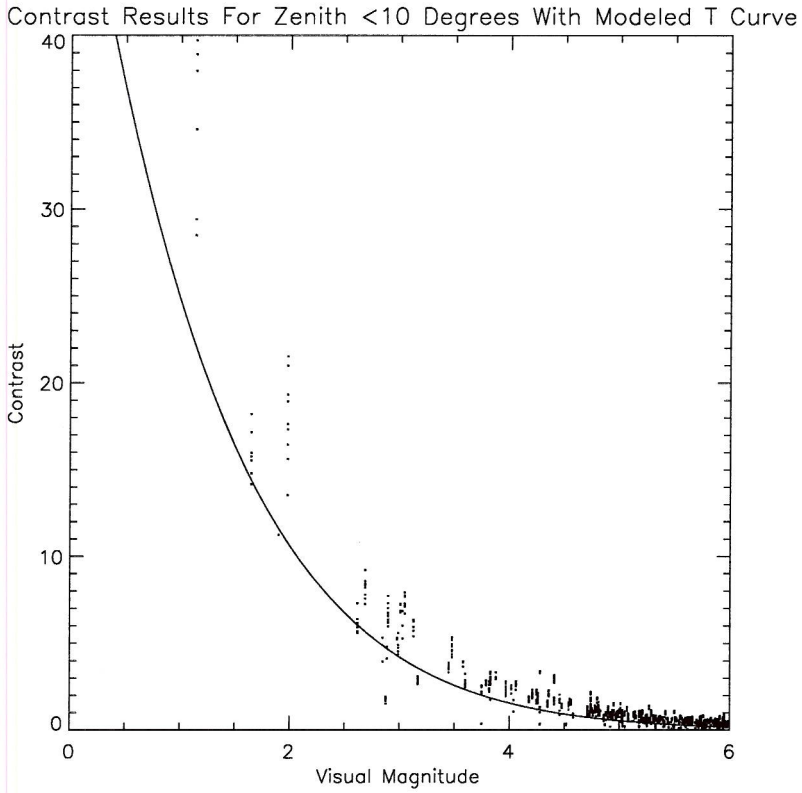

Figure 8. Model shown in upper left plot of Figure 7 compared with star contrast results for near zenith.

As previously mentioned, stray city lights affect a portion of the SOR images, and the cloud-free contrast thresholds given above did not work well for this region. Improved results were obtained by changing τ from 0.6 to 0.25 for azimuth angles in the range 270-360.

Opaque Cloud Thresholds

A simpler approach was taken to determine a threshold scheme for opaque cloud. For low magnitudes, contrast for a star covered by opaque cloud is much lower than that of the cloud-free case. In previous versions of the algorithm, opaque cloud was identified using a constant contrast threshold of around 0.2. Since there is some variability in contrast with zenith angle, an opaque cloud contrast threshold model was developed using the 80^{th} percentiles of overcast contrasts using data from multiple images with complete cloud cover. Figure 9 shows

that contrast for the opaque cloud case increases rapidly beyond 60° then drops back down beyond 80°. These data were modeled using a seventh degree polynomial. For cases with moon in the field of view, opaque cloud contrasts were lower, as shown in the example plot for full moon. Both models handled low zenith angles poorly, which is an issue that has yet to be addressed. The opaque cloud contrast model may be seen near the bottom of each plot in Figures 4-6.

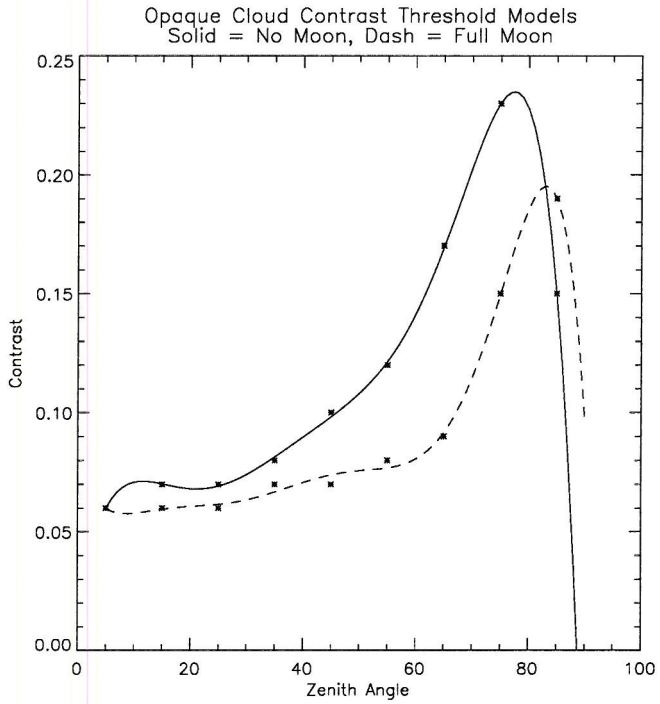

Figure 9. 80th percentiles of star contrast in opaque cloud images as a function of zenith angle. Solid line represents no moon case. Dash line represents full moon case.

Cloud-Free Background

A median cloud-free background image was produced using a single night of cloud-free images, as shown in Figure 10. It was found that for the regions of an SOR image not affected by the stray city lights, the cloud-free background was relatively constant out to about 60°, then increased rapidly out to the horizon. For the region affected by stray city lights, the background values begin increasing beyond 40°. Background values for overcast cases were typically higher, at least out to a zenith angle of 60°. As an added check to determine whether a star is cloud-free, a final threshold based on these results is used. Figure 11 shows the models for azimuth angles < 270° (no city lights) and for azimuth angles > 270° (city lights). If a star is found to be cloud-free based on the earlier contrast threshold check, it must also have a background value less than that given by the cloud-free model. If it does not, the star is classified as being covered by thin cloud. Because moonlight affects the background sky

differently depending on where the moon is in an image, it is difficult to model that affect. Therefore, this test is only used for the no-moon case.

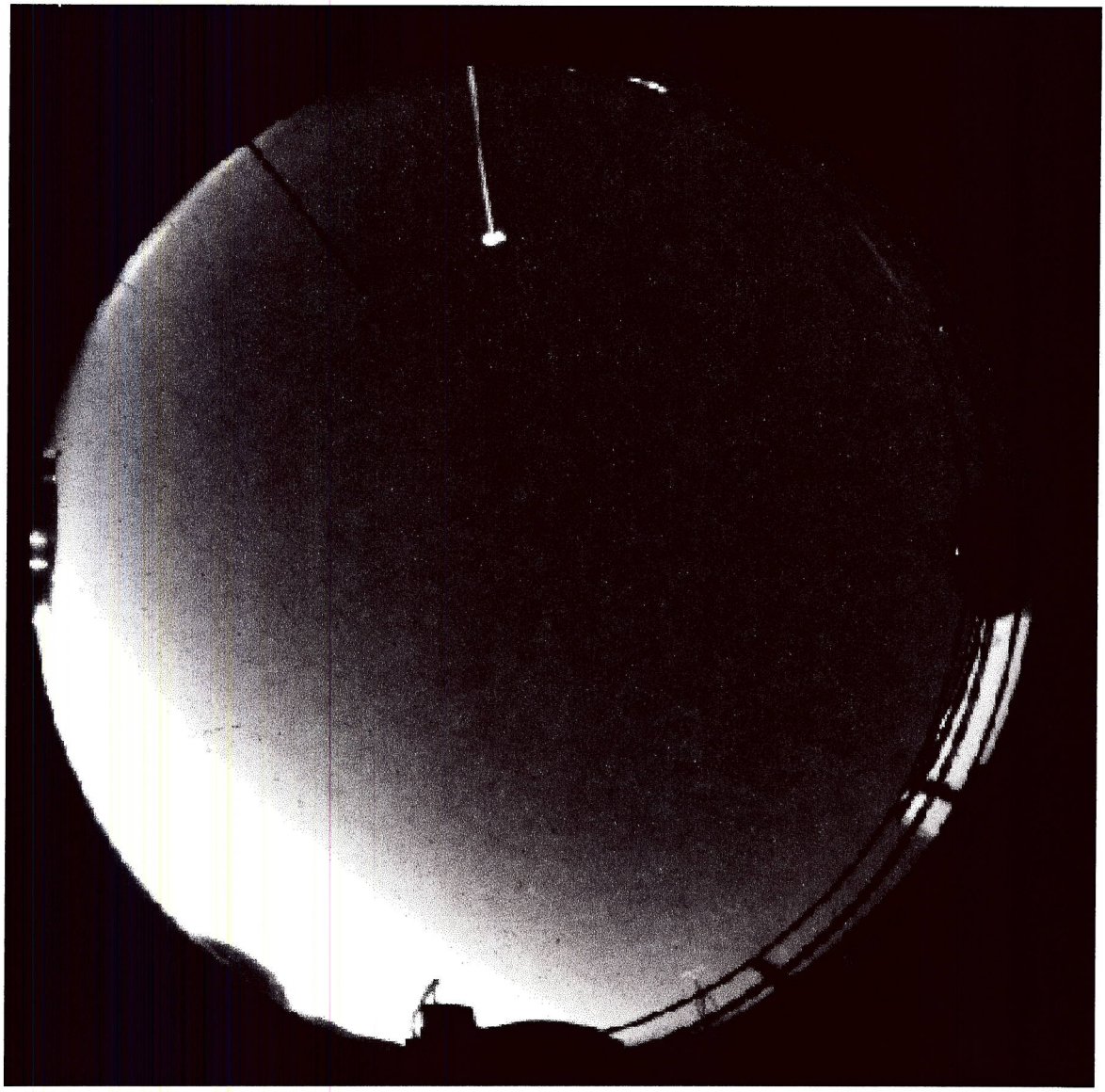

Figure10. Median cloud-free background image for SOR created using multiple cloud-free images from February 14, 1999.

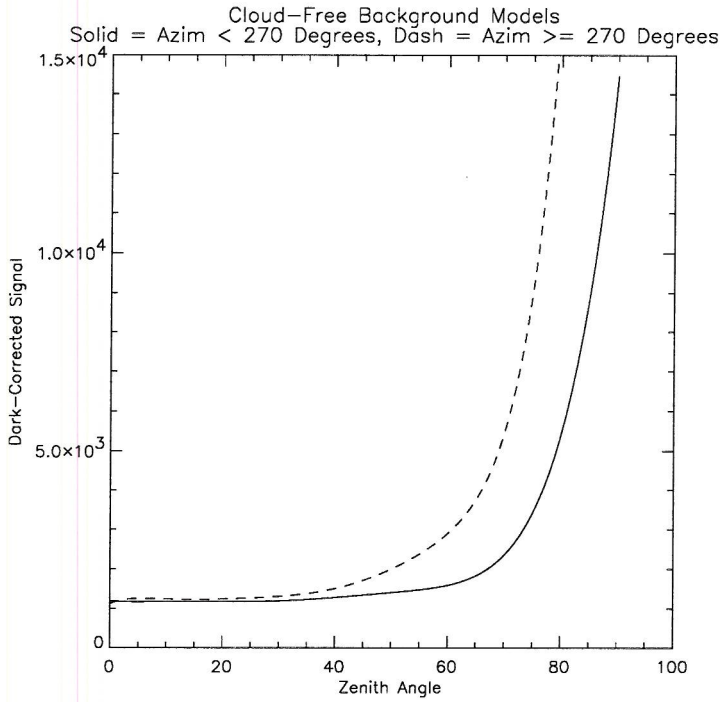

Figure 11. Cloud free background models determined using image in Figure 10.

Summary of Thresholds

Summarizing the steps taken to classify each star, the star is first given an initial classification based on the Gaussian best-fit result, as described in Memo AV99-044t. Next, T, the contrast threshold at zenith is determined using the model appropriate to the moon phase. Then the cloud-free contrast threshold is found using T and Equation 1, where τ is 0.6 in regions of the image not affected by city lights, otherwise it is 0.25. Next, the opaque cloud threshold is determined using the appropriate model for the moon phase. Lastly, if it is a no-moon case, a cloud-free background threshold is determined. Stars with contrasts above the cloud-free contrast threshold with a background value below the cloud-free background threshold (no-moon case) are classified as cloud-free. If these tests fail, the contrast is compared with the opaque cloud contrast threshold. If the contrast is below this threshold, the star is classified as being obscured by opaque cloud. If the contrast is above the opaque cloud threshold, then the star is classified as being obscured by thin cloud.

Sample Algorithm Results

Figures 12-16 show results for different moon phases and cloud conditions. The first three cases are for no moon, and show cloud-free, opaque cloud, and partly cloudy (thin and opaque) masked images. The no moon cases do well, especially when the sky is either completely clear or completely cloudy. When partly cloud regions appear, there are some problems with the resolution of the grid system used and the current method for classifying a

grid cell as cloud-free, opaque cloud-covered, or thin cloud-covered (see Memo AV99-044t). Miscalls are common near the horizon, but that is expected, as opaque cloud contrasts tend to mingle with cloud-free contrasts there. Using simple thresholds makes classifying the horizon areas very difficult. In the cloud-free case under significant moonlight, the algorithm successfully identifies much of the cloud-free regions, as long as they are away from the moon disk itself. As the moon moves toward the horizon, results for cases such as this improve greatly. In the last image set, the sky is almost completely covered with thin cloud, as well as some opaque cloud, and the moon is full and near the center of the image. This is a complicated as most images get. The algorithm successfully identifies about half the thin cloud away from the horizon, identifying the rest as either opaque cloud or cloud-free. Thin cloud near the moon disk is often identified as being opaque cloud. Additional tweaking of thresholds may improve these results, as little time was available to test the algorithm prior to delivery.

Conclusion

The primary task under this contract was to deliver a nighttime cloud algorithm that would perform under all moon phases and identify cloud-free regions and both thin cloud and opaque cloud. Previous versions of the software could only be used for no-moon cases, and classifications were limited to either cloud-free or overcast. Many different paths could have been taken when designing a threshold technique to classify images according to the above requirements. The particular method used here works reasonably well in uncomplicated images (completely cloudy or clear), as those were the images used to develop the thresholds. As images get more complex, the results may be poor, particularly under moonlit conditions. By spending some time looking at results and modifying the threshold technique, it is very likely that the algorithm could be fined tuned to perform better. It is also unlikely that all issues can be addressed, especially when dealing with moonlight. Attempts to incorporate moon to star distance into the thresholds has yet to prove fruitful.

We were pleased with these results, considering that it was the first night algorithm to be fielded. The results appear to be reasonably good, although clearly further research would benefit this work. Current work involving the extraction of optical depth from calibrated images shows promise as something that could be incorporated into the next generation of cloud identification in nighttime WSI imagery. This new work is based on fully calibrated imagery. The use of the calibrated imagery holds potential for better classification of the expected star signal, as well as better classification of the expected background. In addition, use of absolute radiance provides potential for developing and interpolation scheme to assess cloud cover at higher spatial resolution.

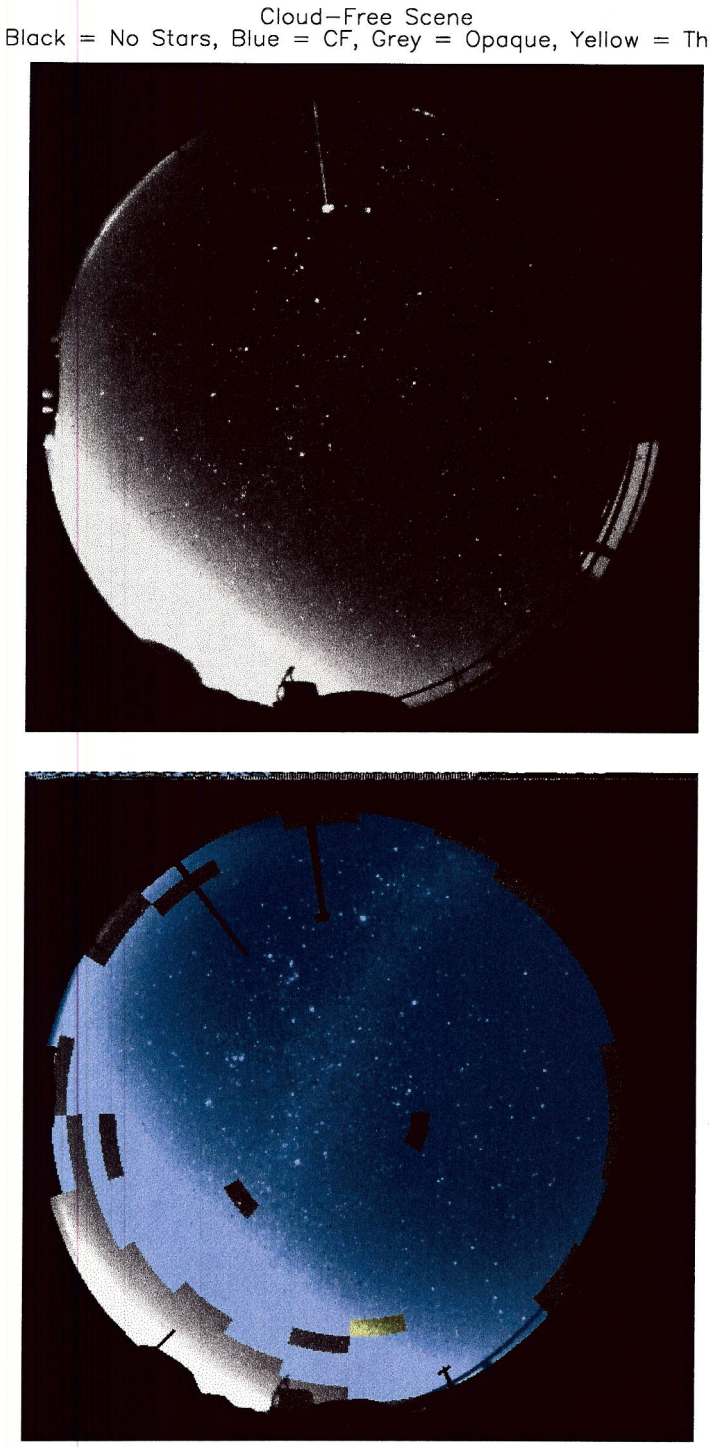

Figure 12. Cloud decision mask for cloud-free, no-moon SOR image collected on February 14, 1999.

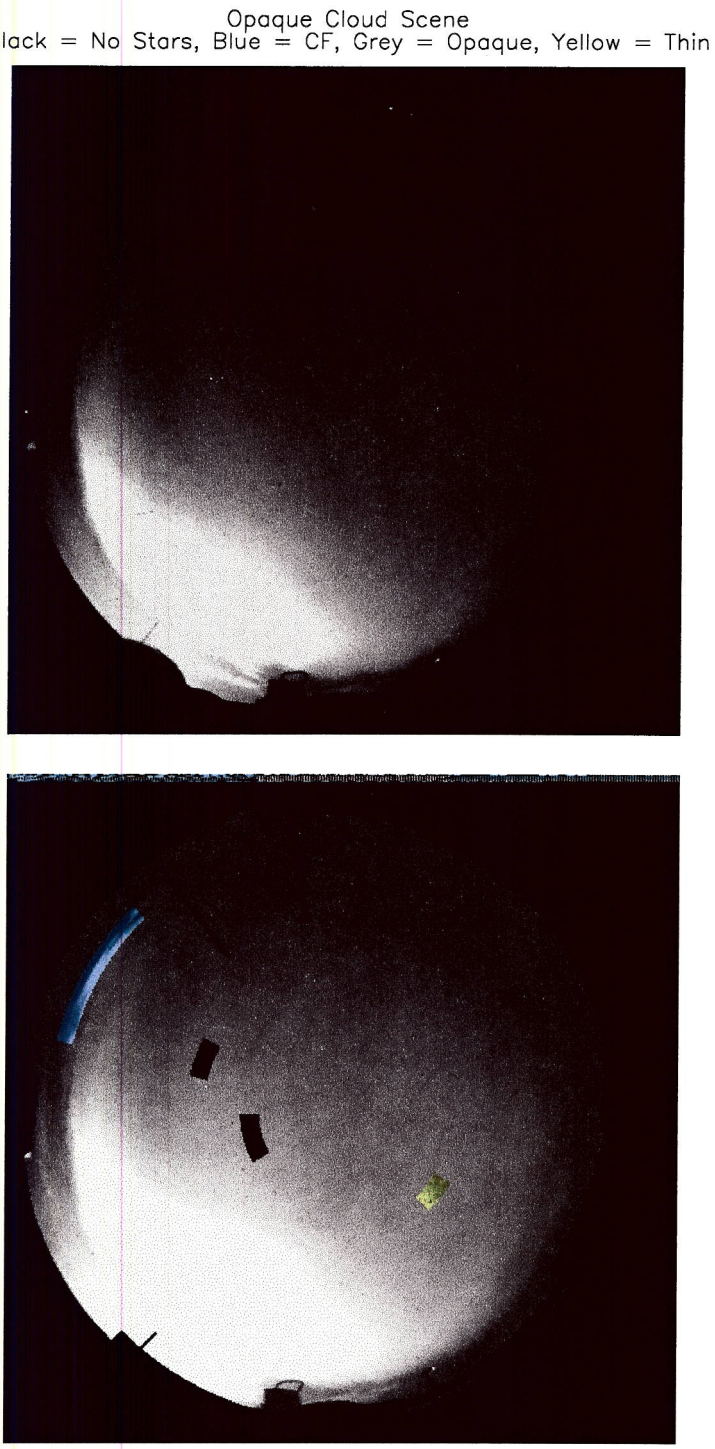

Figure 13. Cloud decision mask for opaque cloud-covered, no-moon SOR image collected on June 16, 1999.

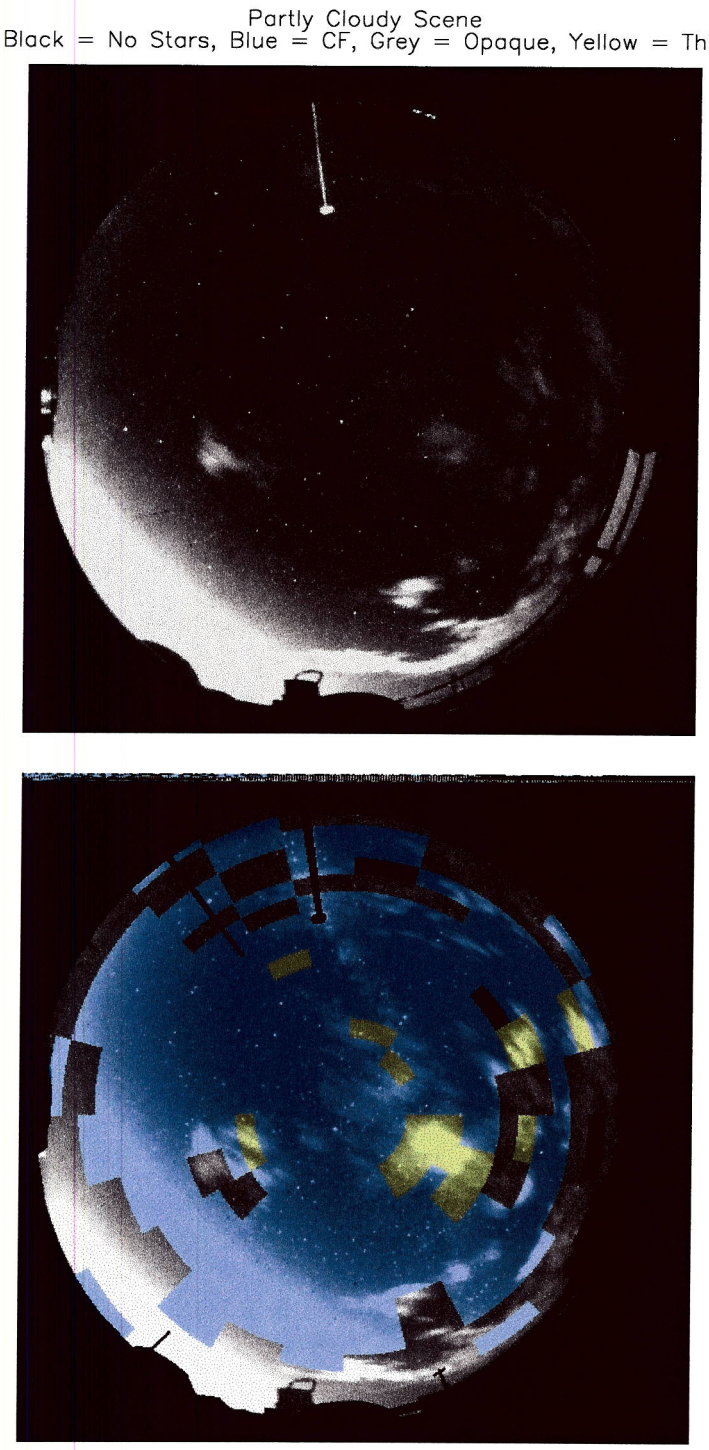

Figure 14. Cloud decision mask for partly cloud-covered, no-moon SOR image collected on June 20, 1999.

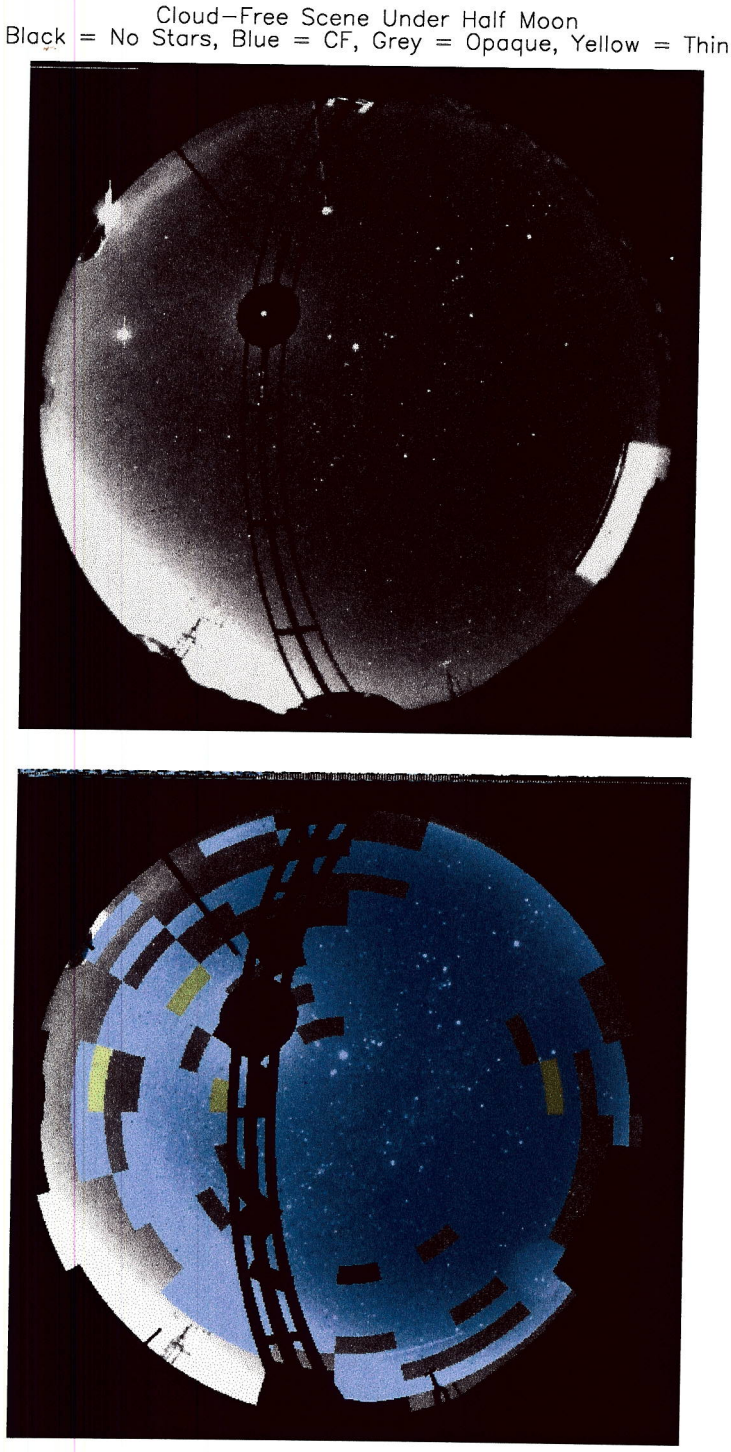

Figure 15. Cloud decision mask for cloud-free, half moon SOR image collected on February 1, 2001.

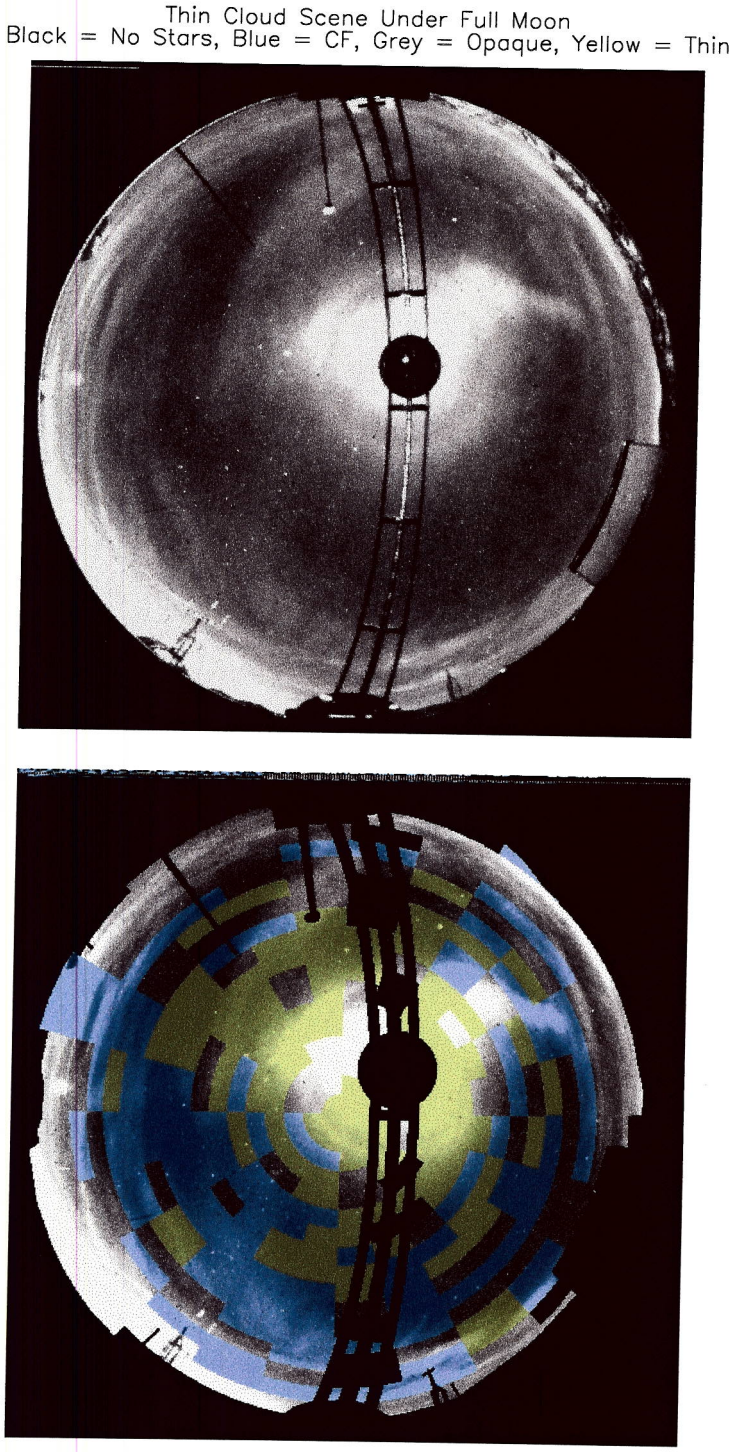

Figure 16. Cloud decision mask for thin cloud-covered, full moon SOR image collected on February 5, 2001.